



# Investigation of groundwater potential and groundwater pollution risk using the multi-criteria method: a case study (the Alaşehir sub-basin, western Turkey)

Ali Can Demirkesen<sup>1</sup> · Seda Budak<sup>1</sup> · Celalettin Şimşek<sup>2</sup> · Alper Baba<sup>3</sup>

Received: 24 May 2019 / Accepted: 25 April 2020 / Published online: 19 May 2020  
© Saudi Society for Geosciences 2020

## Abstract

Determination of the groundwater potential (GWP) and groundwater pollution risk (GWPR) areas is a very important tool in the semi-arid regions in the world. Like many countries in the world, most of the major settlements in the cities of Turkey are located in permeable alluvial plains. Therefore, significant groundwater pollution is encountered in an alluvial plain containing settlements and industrial sites. This study focuses on the determination of the GWP and GWPR areas in the Alaşehir sub-basin, which is one of the economically important districts of the Aegean region, located in the Gediz River basin in western Turkey. In this study, the GWP and the GWPR areas were identified and a GWP index map was generated. The GWP areas in the study basin were determined using different proxies as a multi-criteria method based on geographic information system (GIS) integrated with remote sensing (RS). The result of the study indicates that the most GWP locations in the basin are seen in the west and southeast of the study region. Based on these results, it is understood that the significant GWP and GWPR areas are near the big settlement districts such as Alaşehir and Salihli. In particular, the 115-ha organized industrial zone located in the Salihli district is an important factor of the potential for consuming and contaminating water resources. This study method is so important for the selection of both city and industrial areas as well as for regional environmental planning in terms of the GWPR management.

**Keywords** Groundwater resources · Pollution risk · Multi-criteria method · DRASTIC methods · Gediz River basin

Responsible Editor: Broder J. Merkel

✉ Ali Can Demirkesen  
ademirkesen@yahoo.com

Seda Budak  
sbyo1993@gmail.com

Celalettin Şimşek  
celalettin@deu.edu.tr

Alper Baba  
alperbaba@iyte.edu.tr

- <sup>1</sup> Department of City and Regional Planning, İzmir Institute of Technology, İzmir, Turkey
- <sup>2</sup> Department of Drilling Technology, Torbalı Technical Vocational School of Higher Education, Dokuz Eylül University, İzmir, Turkey
- <sup>3</sup> Dept. of Civil Engineering, İzmir Institute of Technology, İzmir, Turkey

## Introduction

Planning a city has a close relation to social and economic structures, land use/cover (LULC), and physical earth structures affecting the city. Unplanned cities, which are developed with avoiding these parameters, cause adverse effects on both humans and their environment. It is important to minimize the adverse impacts that may occur in the planning of areas such as housing and residential areas, industrial facilities (waste storage, energy production, etc.), and agricultural areas as well as managing natural resources (Velibeyoğlu et al. 2018; Hayat and Baba 2017; Zhao et al. 2017; Qiao et al. 2018). Providing this will only be possible by determining and evaluating all kinds of information and the existing natural resources of the urban area. Although the groundwater resource is one of the most important natural resources, the importance of planning has not been noticed for a long time, because it is not visible like other natural resources above the ground. The groundwater resource and its pollution risk directly or indirectly affect

all species living around them. Therefore, it is also directly related to urban development. This relationship, which has been on the agenda with the acceleration of urban development in the 1900s, still plays an important role today (Frans 1999; Carmon et al. 1997).

Determination of the GWP is associated with multi-proxies. This situation requires the necessity of a multi-criteria decision-making method. When this situation is considered, it is the main problem to consider which multi-criteria decision-making method is the most appropriate for the study. Then, the proxies required for the analysis of the GWP are determined and the weights of each identified proxies are determined depending on the impact on the GWP analysis. Another important stage is to check whether the geo-information obtained as a result of the operations are efficient and accurate or not. Finally, in the light of the geo-information obtained, it is expected that the current LULC will be compared and examined and that it will be able to produce robust decisions for future developments. There are many multivariate studies used to determine the GWP. One of the examples of these studies is the work done by Ramu and Vinay in Karnataka in 2014. In this study, they used a GIS-based multi-criteria method to determine the GWP. In the study, nine different variables were used. These proxies (parameters, variables) can be listed as drainage density, elevation, geology, geomorphology, LULC, lineaments, dykes, rainfall pattern, slope gradient, and soil texture. Also, in this study, Saaty's analytic hierarchy process (AHP) (Ramu and Vinay 2015; Saaty 1980, 2008, 2012) was used to determine the effects of variables.

Similarly, Fashae et al. (2013) investigated the GWP in Southwest Nigeria with using multi-criteria decision analysis. The variables used in this study are geology, rainfall, geomorphology, soil, drainage density, lineament density, land use, slope, and drainage. Also, Mandal et al. (2016) conducted a study using a similar multi-criteria decision analysis technique in the basin of the Balasore region of India. Waikar and Nilawar (2017) used GIS and RS techniques to determine the GWP in India. They have used six parameters. These include geomorphology, slope, drainage density, lineament density, LULC, and geology. To identify the GWP, they have divided the final map into five categories: excellent, good, moderate, poor, and very poor.

One of the variables that are the most related to the groundwater is vegetation. Normalized Difference Vegetation Index (NDVI), which is an important part of this study and which can be obtained by RS techniques, is data information that is commonly used in the groundwater and surface water detection. Fu and Burgher (2015) analyzed the 23-year period variation of climatic factors and groundwater in the study of semi-arid riparian fields in the Naomi Bvadasin of Australia. They used Landsat-7 and Landsat-5 satellite imageries (image bands) between 1987 and 2010 to make NDVI calculation.

In another study that focused on the NDVI variable, Ardakani and Ekhtesasi (2016) used GIS and RS techniques, too. They used five basic parameters to determine the GWP. These parameters can be listed as lithology, geomorphology, slope, NDVI, and NDWI. They created a thematic map for each parameter and divided each map into four classes including "very good," "good," "moderate," and "poor." They used QUEST (Quest: unbiased and efficient statistical tree) (Huajie et al. 2016) to determine how and what effect each variable will have on the resultant map. As a result, a thematic map of the Chaoyang Province, which provides insight on the GWP, was created. Besides, similar to this study, Dhar et al. (2015) performed a hydro-environmental assessment of a regional groundwater aquifer: HiraKud command area in India.

Another important variable in the literature is hydraulic conductivity. Although this variable is more commonly used in the detection of groundwater pollution risk areas, it is said to have a significant effect on the GWP. Ahmed et al. (2017) used a DRASTIC model which is a type of method to determine the groundwater pollution potential in Saudi Arabia. Expansion of the word DRASTIC includes depth to groundwater, recharge, aquifer media, soil media, topography, the impact of the vadose zone, and conductivity. The DRASTIC model is a multi-criteria decision method that is very often used to detect the GWP presence and potential pollution hazards. Barış (2008) used the DRASTIC model to determine groundwater pollution risk and integrated water quality in the Tahtalı Dam basin. In addition, Atlı (2010) used the DRASTIC model to determine the groundwater pollution risk in the Erzin plain. In this study, in addition, RS methods such as NDVI and MNDWI were used together. Unlike previous studies, in this study, more variables were used and each variable was classified and visualized by assigning the GWP index values from 1 to 5 where 1: very low; 2: low; 3: moderate; 4: high; and 5: very high. A weighted image overlay process was also employed for each variable to process multi-criteria decision-making. Also, no other studies related to city planning have been found in the studies on this subject. In this sense, this study can be also regarded as a pioneering work for urban planning to manage the groundwater resources and their pollution risk.

The objective of this study is to provide a multi-criteria weighted overlay method for determining the groundwater potential (GWP) and groundwater pollution risk (GWPR) areas in the alluvial plain. The area chosen for the study is the Alaşehir sub-basin, located in the Gediz River basin in western Turkey, because this area has a rich GWP with an aquifer under fertile agricultural alluvial soils and it is also under the GWPR due to industrial settlements over there. This study involves the determination of the GWP by considering multi-proxies as multi-criteria used by a weighted image overlay analysis (Demirkesen and Evrendilek 2017). A multi-criteria evaluation approach is required to incorporate more

than one proxy into the analysis. For this purpose, the method to be used in this study is a multi-criteria decision-making method. This method is based on geographic information system (GIS) integrated with remote sensing (RS). As a result of the research, all the ten proxies were decided and selected to be employed in the analysis. Each proxy was examined in terms of its impact on determination of the GWP, and finally, with a combined evaluation of all the ten proxies, a conclusion was made on the GWP of the Alaşehir sub-basin. Then, the GWPR areas were interpreted and discussed. In conclusion, the results and findings seem to be satisfactory and consistent with both the previous studies and the available existing geo-information.

In this study, the GWP and GWPR areas were identified and a GWP index map was generated. The GWP areas were determined using different proxies as a multi-criteria method based on geographic information system (GIS) integrated with remote sensing (RS). The method used in this study includes 10 proxies that play important roles on the determination of the GWP areas: (1) normalized difference vegetation index (NDVI), (2) modified normalized difference water index (MNDWI), (3) land use/cover (LULC), (4) lineament, (5) topography (digital elevation model—DEM), (6) slope, (7) drainage, (8) lithology, (9) hydraulic conductivity, and (10) soil types.

The study shows the significant GWP and GWPR areas are near the big settlement districts such as Alaşehir and Salihli. In particular, the 115-ha organized industrial zone located in the Salihli district is an important factor of the potential for consuming and contaminating water resources. The study method is therefore so important for the selection of city and industrial areas as well as regional environmental planning in terms of the GWPR management for future studies.

### The study area

The study area, the Alaşehir sub-basin, is one of the five sub-basins of the Gediz River basin, located in the western Turkey (Fig. 1). The Gediz River basin covers an area of 1,713,697 ha and is located between 38° 04'–39° 13' north latitudes and 26° 42'–29° 45' east longitudes.

The Mediterranean climate type is seen in the Alaşehir Basin, a sub-basin of the Gediz River basin. The average temperature of the basin is about 15 °C in winter. The average temperature difference is about 30 °C in summer. According to the observations of the meteorological station in the basin, the total annual rainfall ranges from 450 to 800 mm. Summers are dry and winters are rainy. Most of the rain falls during the winter season (DSI 2016; COB 2008).

### Geology of the study area

The basement of the Gediz River basin is the Paleozoic-aged Menderes Metamorphic consisting of gneiss, schist, and

marble (Baba and Sözbilir 2012). The Neogene sedimentary layer overlays the basement rocks with unconformity in the study area (Fig. 2). The Alaşehir Plain is full of Neogene sedimentary rocks that contain sandstone, conglomerate, claystone, limestone, and volcanic layers (Seyitoğlu et al. 2000). Quaternary-aged unconsolidated sediments cover these units along the plain. This alluvium material consists mostly of gravelly and clayey sands (Rabet et al. 2017).

The marble layers in the metamorphic series are highly permeable and considered to be geothermal reservoir rock in the study area. The Neogene sediments consist of sedimentary layers including sandy clayey levels with low permeability layer. Especially, claystone levels of the Neogene sediments are very thick impermeable layers for the geothermal system. The permeability of the alluvial layer is changing depending on the material properties. Especially, the west coast of the plain has a very high permeability where it contains sand and gravel sediments.

The alluvial layer is the most important and most suitable aquifer for groundwater resources. Groundwater is provided by shallow wells with depths ranging from 120 to 150 m from this aquifer. The groundwater discharge rate of these wells is ranged from 5.0 to 30 L/s (Özen et al. 2012; Baba et al. 2016; Rabet et al. 2017). The general groundwater flow direction in the alluvial aquifer system is from west to east. The groundwater flow path is determined by the alluvial sediments with a high permeability value.

### Vegetation of the study area

In Fig. 3, showing an infrared false-color composite image, RGB = 754 in 3-D of Landsat-8 Operational Land Imager (OLI) (2018) satellite image bands acquired in September 2017, where forest areas appear in dark green. Agricultural vegetation crops are in both light green and turquoise colors. Bare rocks appear in purple and pink colors. Water bodies such as lakes appear in dark blue. The regions with all types of bright green colors represent healthier vegetation. Purple and pink colors refer to areas that do not contain any vegetation (Barsi et al. 2014). However, in particular, it can be seen that the alluvial soils in the study area are mostly covered with vineyards.

## Materials and methods

### Data processing

In the study, the GWP areas in the Alaşehir sub-basin were determined by using a multi-criteria approach, in other words, a weighted image overlay method that focuses on a GIS method integrated with RS (Demirkesen and Evrendilek 2017), and the accuracy and efficiency of the results obtained at the end of

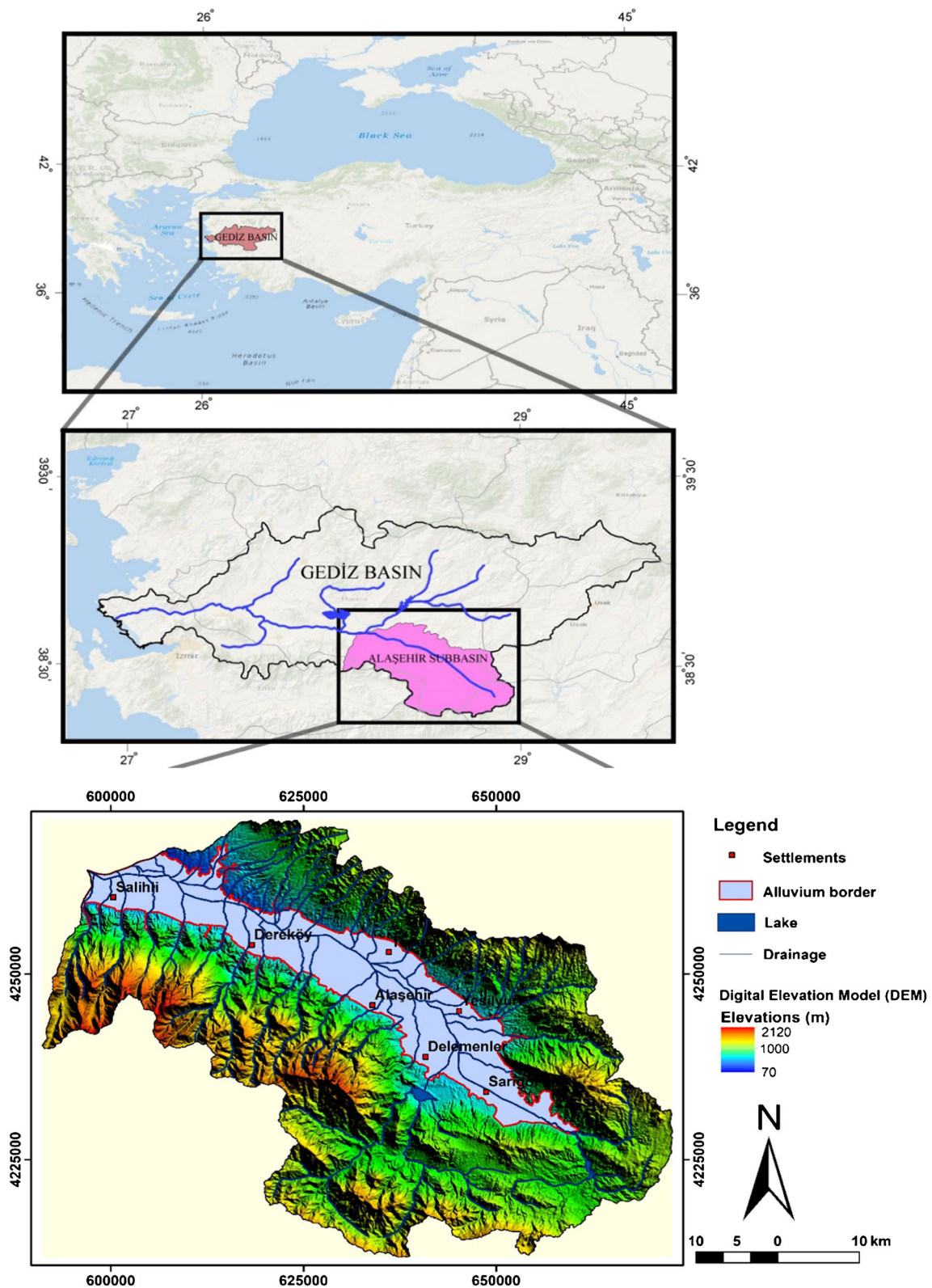


Fig. 1 Location map of the Alaşehir sub-basin in the Gediz River Basin, Turkey

the study were checked. In this context, the data used, the sources of the data, and the procedures applied to the data are summarized in Fig. 4 and Table 1 where ED50 Datum,

UTM Projection with 35N Zone, and 30-m grid size resolution for all kinds of images and DEMs were used for georeferencing.

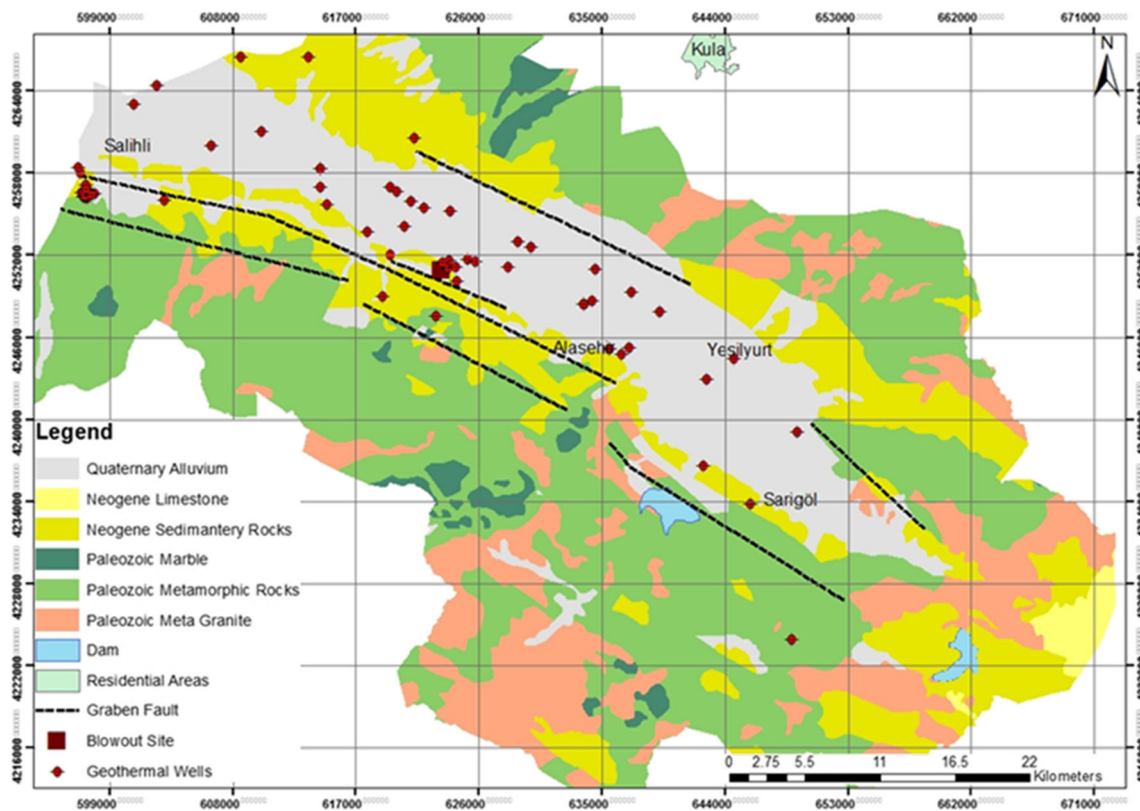


Fig. 2 Geological map of the Alaşehir sub-basin (modified from Rabet et al. 2017)

**Proxies used in the study**

In the study, a multi-criteria approach was used to determine the GWP and its analysis for decision-making. The criteria (proxies, parameters, or variables) that may be most related to the GWP indicators were selected. In order to determine the significant

degrees of weights of the proxies, two studies with similar proxies were inspired by this study. The first of these is the GWP analysis of Waikar and Nilawar in India (2017). The second is the groundwater pollution potential analysis carried out by Ahmed et al. (2017) in Saudi Arabia. The method used to obtain the GWP is expressed by the formula as a weighted image overlay:

Fig. 3 Landsat-8 OLI RGB = 754, a false color composite image in 3-D of the study area, where pink areas: bare rock; dark green areas: forest; light green and turquoise areas: vegetation/crop; and dark blue areas: water body

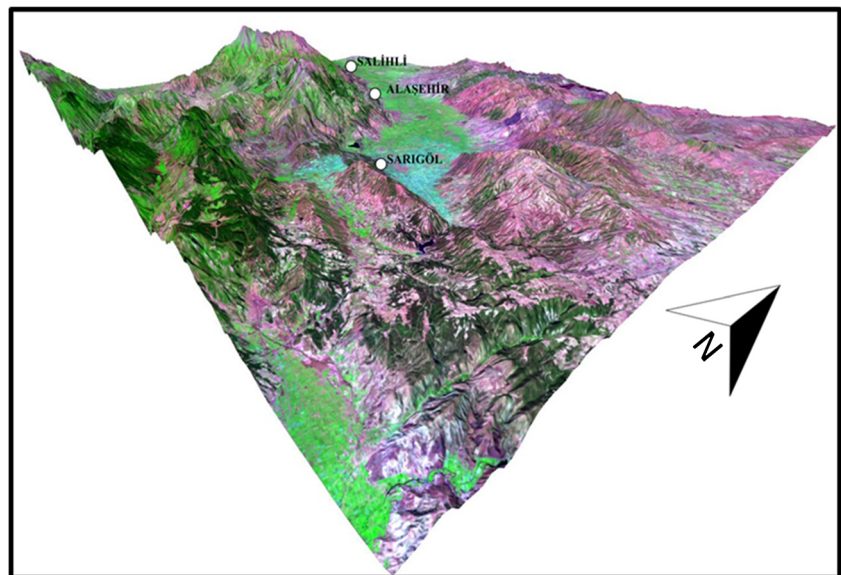
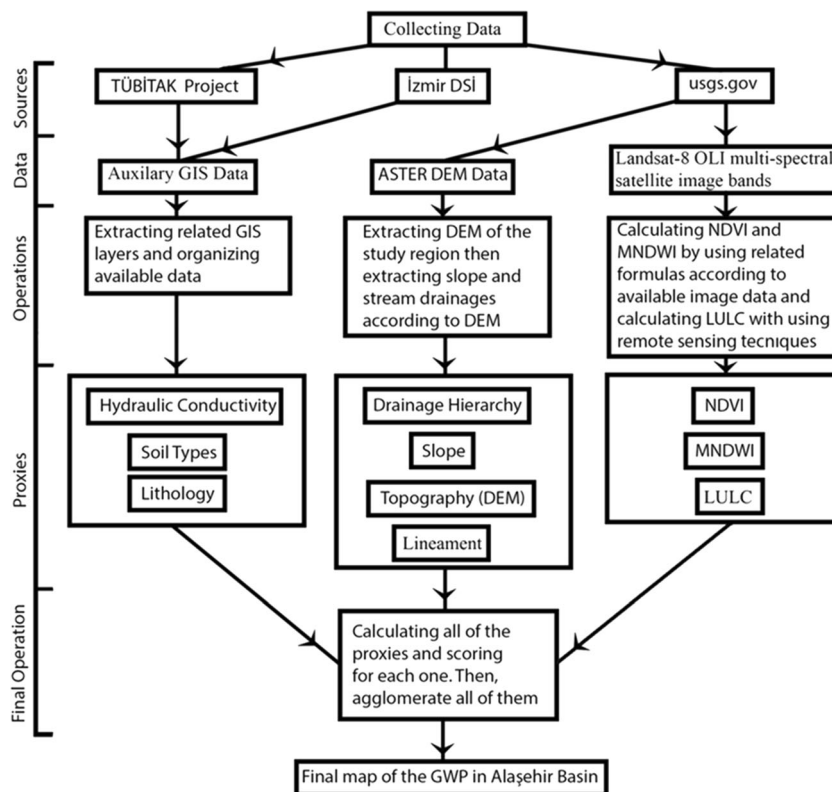


Fig. 4 The data processing diagram



$$GWP = \sum_{i=1}^n W_i P_i = W_1 P_1 + W_2 P_2 + \dots + W_{10} P_{10} \quad (1)$$

where GWP → groundwater potential

$n = 10$  → the number of the proxies.

$P_i$  → proxies.  $i = 1 \dots 10$

$W_i$  → weight coefficients of the proxies, where weight coefficients range from 1 to 5. These range values are assigned as user-defined according to significance to the GWP. All the ten proxies and their weight coefficients were determined by the literature search, and the calculation methods of these proxies are explained later on. The details of the GWP index values and class intervals of the resultant maps can be seen in Table 1, which illustrates the detailed properties of all the ten proxies.

The GWP map was generated by using all the ten proxies and their weights. The weighted image overlay computation of the GWP was performed by the formula below:

$$GWP = \sum_{i=1}^n W_i P_i = 2 * P_{NDVI} + 2 * P_{MNDWI} + 2 * P_{LULC} + 3 * P_{Lineament} + 2 * P_{Topography} + 4 * P_{Slope} + 3 * P_{Drainage} + 5 * P_{Lithology} + 4 * P_{Hydraulic Conductivity} + 2 * P_{Soil Types} \quad (2)$$

### Normalized difference vegetation index—proxy 1

Vegetation can give an idea about the GWP richness. If the amount of the groundwater in the study area is high, this will have a positive effect on the vegetation that continues its development on the alluvial soils in that area. It is possible to observe vegetation dynamics by using RS methods. One of the most common RS methods used for this purpose is NDVI (Normalized Difference Vegetation Index) (Figs. 5, 6, and 7 and Table 1).

- General NDVI formula:

$$NDVI = (NIR - RED) / (NIR + RED) \quad (\text{Huajie et al. 2016}). \quad (3)$$

- For Landsat-8 OLI:

NDVI thematic image map

$$= (Band 5 - Band 4) / (Band 5 + Band 4) \quad (4)$$

- Calculation method: bands obtained from Landsat-8 OLI multi-spectral satellite images were operationalized

**Table 1** Summary of the proxy properties and the final GWP index values

No	Proxy variables	Unit	Year	Sources	Calculation methods	Weights	Class intervals	Index values of GWP	Details for classifications
1	Normalized difference vegetation index (NDVI)	-1 to 1	21 September 2017	Landsat-8 OLI multi-spectral image data	Idrisi Selva / Image calculator tool by NDVI formula	2	< 0	4	Water
							0 - 0.17	1	Bare rock (inactive vegetation)
							0.18 - 0.24	2	Crop type 1 (healthy vegetation)
							0.25 - 0.34	3	Crop type 2 (healthier vegetation)
							0.35 - 0.44	5	Forest type 1 (active vegetation)
							> 0.44	5	Forest type 2 (very active vegetation)
2	Modified normalized difference water index (MNDWI)	-0.69 to 0.29	21 September 2017	Landsat-8 OLI multi-spectral image data	Idrisi Selva / Image calculator tool by MNDWI formula	2	< - 0.25	1	No water
							-0.25 - 0.21	2	Less water
							-0.2 - 0.11	3	Moderate water
							-0.1 - 0.12	4	High water
							> 0.12	5	The highest water
3	Land-use land-cover	Land Use Type	21 September 2017	Landsat-8 OLI multi-spectral image data	Maxlike (multi-spectral image classification) tool was used in Idrisi Selva	2	Settlement	1	Urban and rural settlements
							Bare rock	2	Bare rock
							Crop 1	3	Vegetation type 1
							Crop 2	3	Vegetation type 2
							Forest	4	Forest
							Water	5	Lakes and rivers (water bodies)
4	Lineament	Meters (distances to the lineaments)	2018	Digital elevation model (DEM) and Landsat multi-spectral image of Alaşehir sub-basin / ASTER DEM	Lineaments were determined using ASTER DEM and Landsat multi-spectral image data	3	> 1500	1	Areas furthest to lineaments (the lowest value)
							700 - 1500	2	Low index value
							300 - 700	3	Moderate index value
							100 - 300	4	High index value
							1 - 100	5	Areas closest to the lineaments (the highest value)
5	Topography	Meter (elevations from the sea level)	2018	Digital elevation model (DEM) of Alaşehir sub-basin / ASTER DEM	Idrisi Selva / GIS analysis and classification tool	2	> 1000	1	Very high elevated areas in the region.
							500 - 1000	2	High elevated areas in the region.
							200 - 500	3	Moderate elevated areas in the region.
							120 - 200	4	Low elevated areas in the region.
							52 - 120	5	Very low elevated areas in the region.
6	Slope	Degree	2018	Digital elevation model (DEM) of Alaşehir sub-basin / ASTER DEM	Idrisi Selva / Slope tool	4	> 29	1	Most sloping areas in the region (the lowest value)
							20 - 29	2	Low index value
							10 - 19	3	Moderate index value
							5 - 9	4	High index value
							< 5	5	Least sloping areas in the region (the highest value)
7	Drainage hierarchy	Strahler stream order	2018	Digital elevation model (DEM) of Alaşehir sub-basin / ASTER DEM	ArcGIS / Hydrology analysis tool and buffer operations	3	Other values	1	Sub-tributaries of lower hierarchical drainage
							4th order stream	2	Low index value
							3rd order stream	3	Moderate index value
							2nd order stream	4	The Alaşehir creek (higher index value)
							1st order stream	5	The Gediz river (the highest index value)
8	Lithology	Aquifer type	2018	İzmir DSI GIS layers	Available data were used in ArcGIS	5	Rock type 1	1	Paleozoic units containing local groundwater
							Rock type 2	1	Neogene crushed units containing local groundwater
							Cracked rock	2	Volcanic rocks containing local groundwater
							Karst rock type 1	3	Paleozoic marbles containing local groundwater
							Karst rock type 2	3	Neogene limestones containing local groundwater
							Granular units	4	Alluvial units with extensive groundwater
Water	5	Lakes							
9	Hydraulic conductivity	0 to 46 Meter / Day	2018	TUBITAK project / No: 115Y065	Available data were used in ArcGIS	4	No data	1	No data
							0 - 6	2	Lowest hydraulic conductivity values
							6 - 20	3	Moderate hydraulic conductivity values
							20 - 35	4	High hydraulic conductivity values
							35 - 46	5	Highest hydraulic conductivity values

10	Soil types	Soil type	2018	İzmir DSI GIS layers	Available data were used in ArcGIS	2	No data	1	No data
							8th class soil	5	Water collection area
							7th class soil	2	Very sloping, stony, dry, swamp
							6th class soil	3	Woodland, meadow, very sloping, wet or too dry
							5th class soil	5	Stiffness and wetness, flat land
							4th class soil	3	Very sloping, poor drainage
							3rd class soil	4	Medium slope, low water retention capacity
							2nd class soil	4	Low slope, medium thick soil
							1st class soil	5	1% less slope, loamy, good water holding capacity.
							11	Sum of groundwater potential maps/images	Class index value
51 - 65	2	Low vulnerable for groundwater							
66 - 80	3	Moderate vulnerable for groundwater							
81 - 95	4	High vulnerable for groundwater							
> 96	5	Very high vulnerable for groundwater							

according to the formula by the image calculator tool in Idrisi Selva system (2018) which is software of RS integrated with GIS.

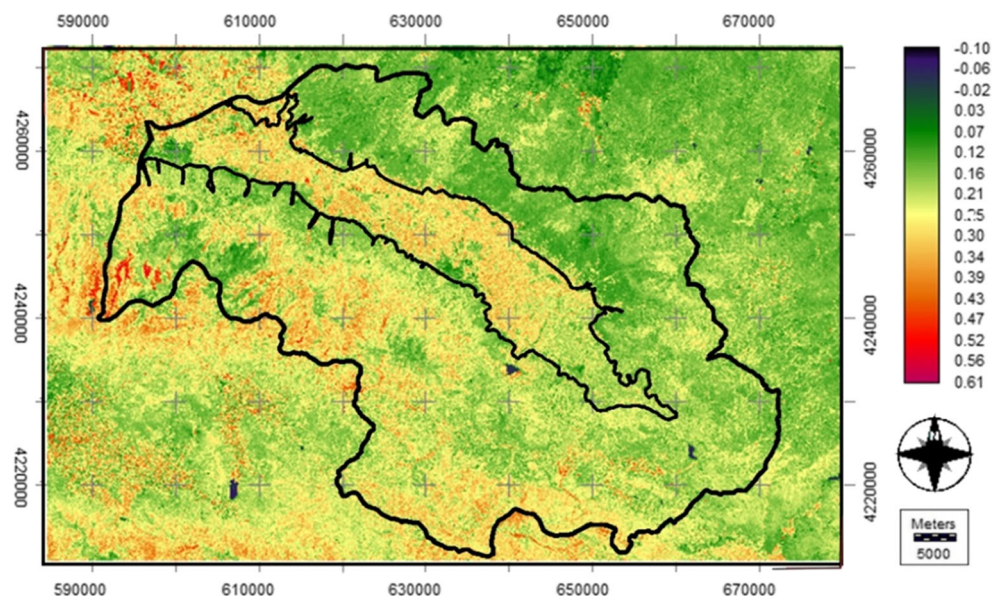
- In our case, in the classification of the NDVI image: 0–0.17 was assigned to the GWP index value 1 due to bare rock (inactive vegetation); 0.17–0.24 was assigned to the GWP index value 2 due to crop type 1; 0.24–0.34 was assigned to the GWP index value 3 due to crop type 2; 0.34–0.44 was assigned to the GWP index value 5 due to forest (active vegetation); bigger than 0.44 was assigned to the GWP index value 5 due to forest (very active vegetation). In classification of the NDVI image, less values than zero (i.e., negative values) were assigned to 4 as the GWP index value because there is no vegetation, but water bodies.

Basically, NDVI is dependent on the reflectance of the infrared rays of the vegetation in a region. Green leaves, which

are healthy and denser, reflect near infra-red (NIR) band energy and absorb the red light (red band) by means of the chlorophyll which prevents the plant from overheating (Fu and Burgher 2015). In an unhealthy vegetation, this will be the opposite. In an area, when the NDVI formula is applied, higher values will express a healthier vegetation. NDVI values vary ranging from  $-1$  to  $+1$  and NDVI (Fig. 5). Negative values can be identified with the water surface (Jin et al. 2011).

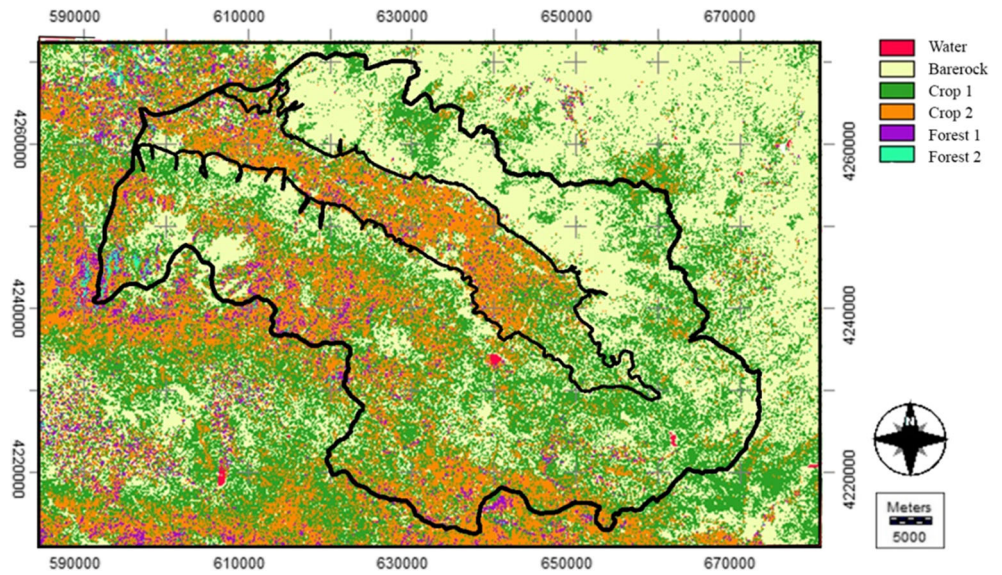
As the NDVI value decreases, the GWP decreases. Considering this, the highest NDVI values were assigned as 5 points of the GWP index value and the lowest NDVI values were assigned as 1 point of the GWP index value. However, as the negative values indicate lakes and surface water deposits, negative values were assigned as 4 points as exceptional. The weight coefficient of the NDVI proxy was assigned as 2 ( $W_1 = 2$ ) according to significance to the GWP (Figs. 5, 6, and 7 and Table 1).

Fig. 5 NDVI thematic map





**Fig. 6** Classification of the NDVI thematic map (Fig. 5) with the defined legend of LULC



**Modified normalized difference water index—proxy 2**

Modified Normalized Difference Water Index (MNDWI) (Figs. 8 and 9) is a RS method like NDVI. The purpose of this index is to distinguish water areas and built-up areas. MNDWI is a modified version of Normalized Difference Water Index (NDWI) developed by Mc Feeters (1996) for the middle infra-red (MIR) band (Xu 2006).

The MIR band used in the MNDWI calculation provides a more pronounced contrast than the NIR band used in the NDWI calculation. The positive values indicate the water areas and the most negative values represent the built-up areas. Soil and vegetation take the remaining values (Xu 2006).

- General MNDWI formula:

$$MNDWI = (GREEN - SWIR) / (GREEN + SWIR) \quad (5)$$

- For Landsat-8 OLI:

MNDWI thematic image map

$$= (Band\ 3 - Band\ 6) / (Band\ 3 + Band\ 6) \quad (6)$$

**Fig. 7** Re-classification of the NDVI thematic map classes (Fig. 6) with the index values of the GWP. Where the legend values indicate 1: very low; 2: low; 3: moderate; 4: high; and 5: very high

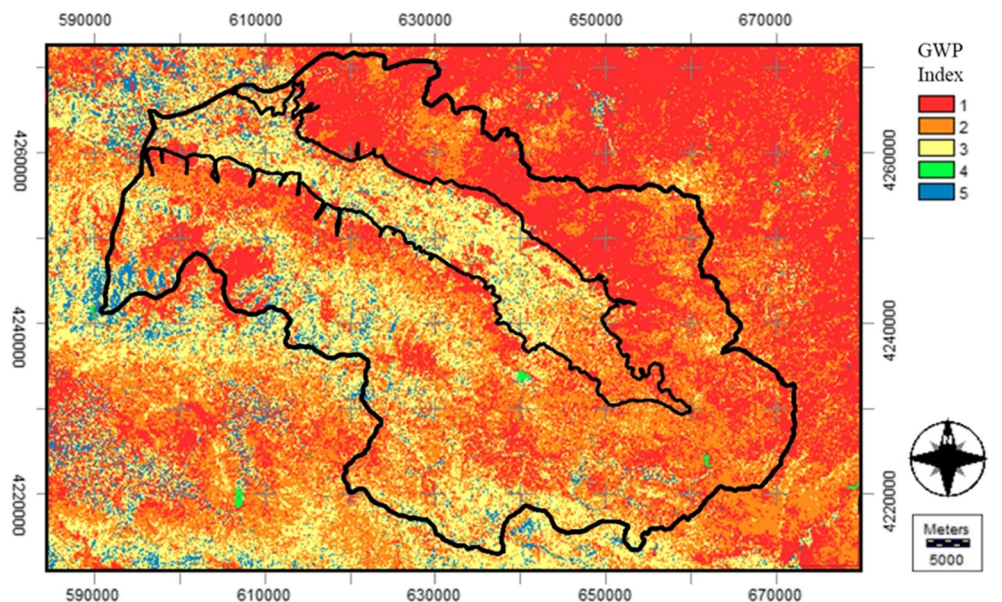
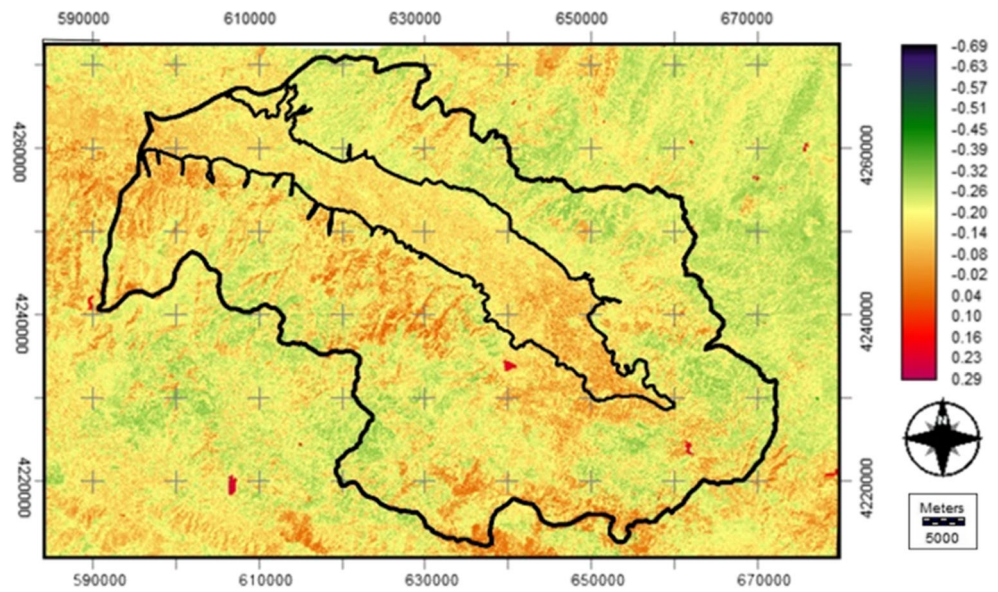


Fig. 8 MNDWI thematic map



- Calculation method: bands obtained from Landsat-8 OLI multi-spectral satellite images were operationalized according to the formula computed by the image calculator tool in Idris Selva software.
- The highest values represent the maximum surface water potential and the lowest values indicate the least surface water potential. For this reason, the lowest-rated pixels were assigned as 1 point as the GWP index value and the highest-rated pixels were scored as 5 points. The weight coefficient of the MNDWI proxy was assigned as 2 ( $W_2 = 2$ ) according to significance to the GWP (Figs. 8 and 9 and Table 1).

**Land use/cover—proxy 3**

Land use/cover (LULC) data (Figs. 10 and 11) gives information about the use of general landfill. Land uses such as the existing settlements, forests, agricultural soils, and surface texture affect the water permeability. Thus, land use/cover provides information about the GWP (Mandal et al. 2016).

Calculation method: the data obtained from Landsat-8 OLI multi-spectral satellite imagery was classified using the maxlike tool in Idrisi Selva software as maximum likelihood supervised classification method (Idrisi Selva 2018).

The areas with the highest GWP are designated as forest and water. The lowest GWP index values were assigned to

Fig. 9 Classification of the MNDWI thematic map (Fig. 8) with the index values of the GWP

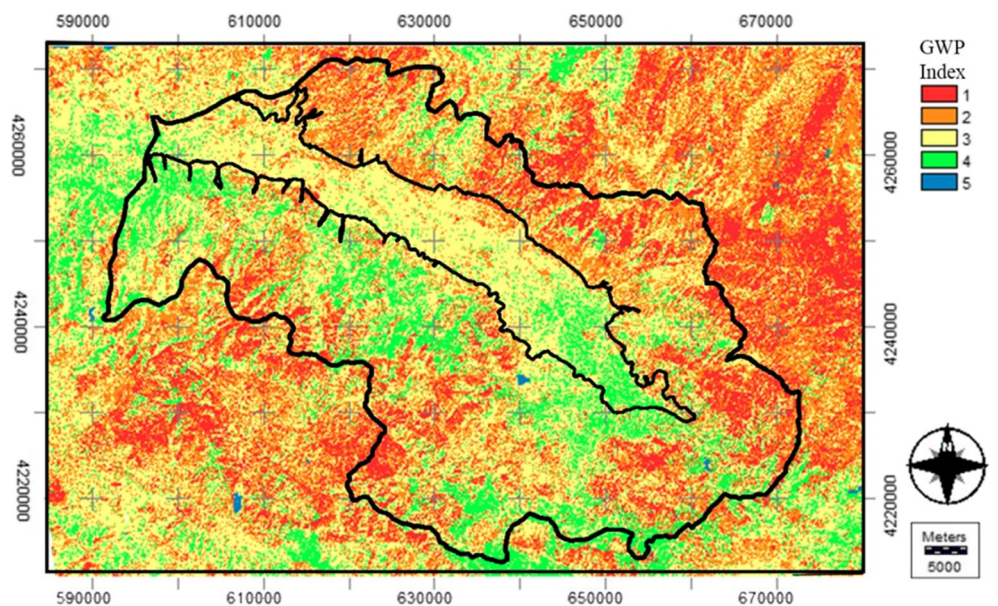
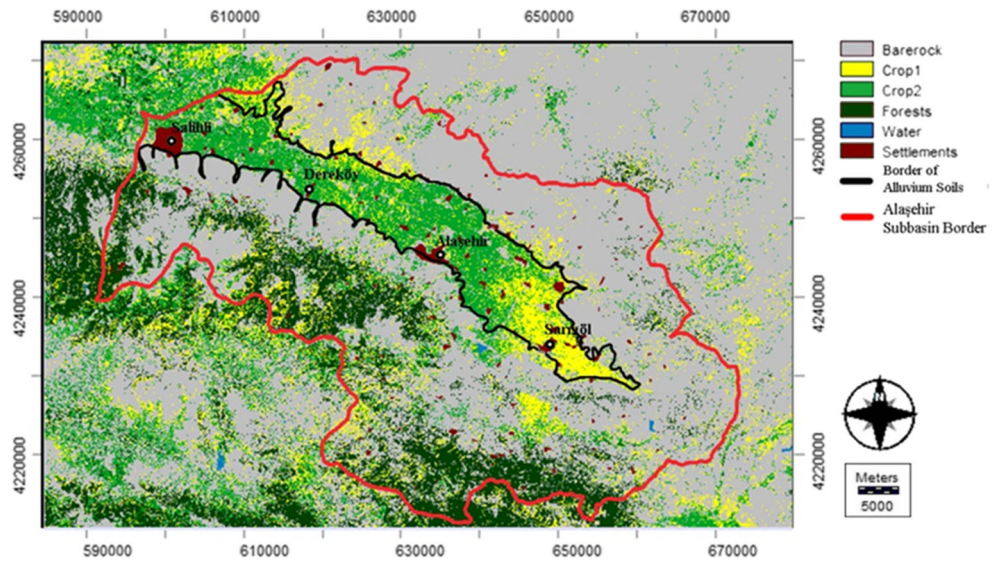


**Fig. 10** Land use/cover (LULC) thematic map



settlements and bare rock areas. The weight coefficient of the LULC proxy was assigned as 2 ( $W_3 = 2$ ) according to significance to the GWP (Figs. 10 and 11 and Table 1).

**Lineament—proxy 4**

Lineaments (Figs. 12, 13, and 14) are seen in rocky regions on the earth. They may occur naturally, such as fault lines, fractures, cracks, drainage networks, and main stream channels. In general, lineaments are caused by increased permeability and porosity in areas exposed to localized weather conditions. Lineaments, due to their high porosity and permeability, are suitable flow areas for groundwater (Ndatuwong and Yadav 2014).

- Calculation method: the shaded Aster DEM and satellite image data were used to determine the lineaments (Fig. 12).
- The proximity to lineaments refers to an increase in the GWP. For this reason, the GWP index value 5 was assigned to the regions at closest distance to lineaments and 1 point was assigned to the farthest regions. The weight coefficient of the lineament proxy was assigned as 3 ( $W_4 = 3$ ) according to significance to the GWP (Figs. 12, 13, and 14 and Table 1). The distance unit is meter.

**Topography—proxy 5**

The DEM (Figs. 15 and 16) indicates the topography, which controls the surface flow direction and humidity

**Fig. 11** Classification of the land use/cover (LULC) thematic map (Fig. 10) with the index values of the GWP

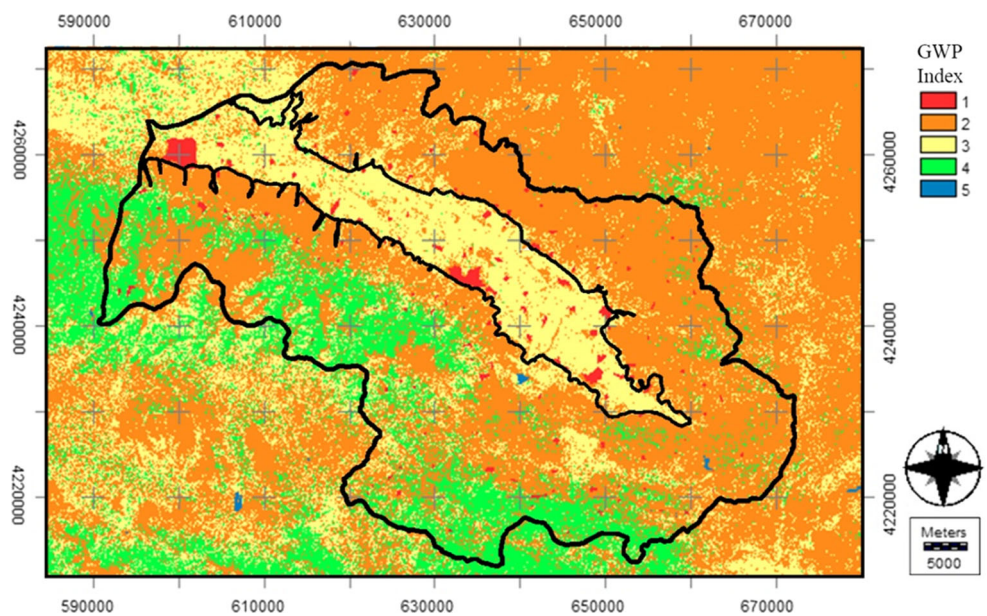
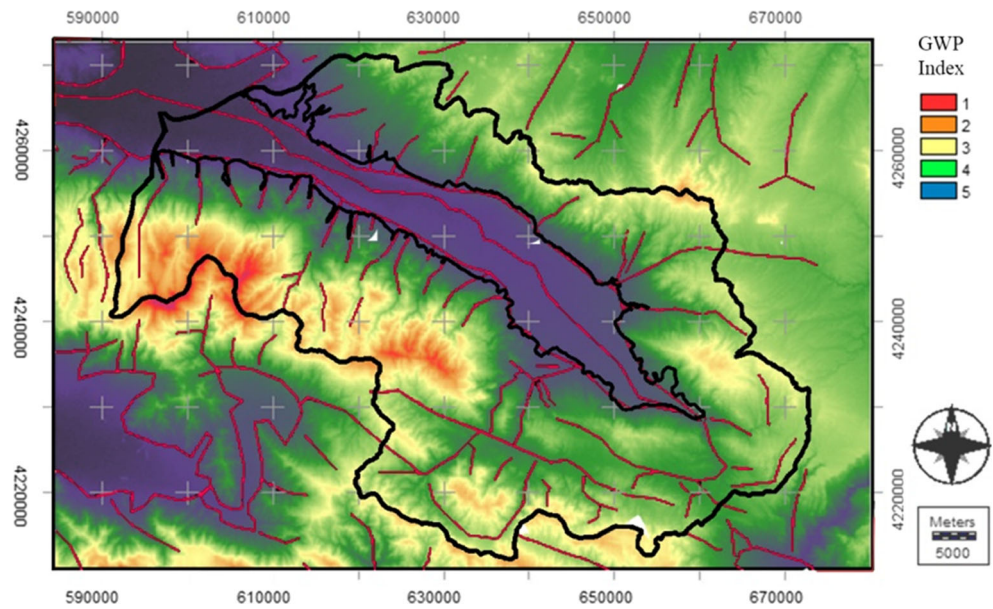


Fig. 12 Lineament thematic map



of a region (Ardakani and Ekhtesasi 2016). When it rains, the water flows from high elevations to lower elevations. Therefore, water tends to accumulate at low heights (Ghodratyabadi and Feizi 2015)

- Calculation method: the Aster DEM data was classified into the five GWP index values by considering the elevations that show the topographic characteristics, indicating sudden changes in elevations and slopes (Figs. 15 and 16).
- In this proxy, the GWP index value 5 was assigned to the lowest elevations (heights) and the GWP index value 1 was assigned to the highest elevations. The weight coefficient of the topography proxy was assigned as 2 ( $W_5 = 2$ )

according to significance to the GWP (Figs. 15 and 16 and Table 1). The elevation unit is meter.

**Slope—proxy 6**

The slope degree (Figs. 17 and 18) has impacts on the flow of water and the discharge into groundwater. It causes the soil surface to be too inclined and the water to flow without being absorbed by the soil. Thus, the surface water in the sloping areas is not stored too much. Therefore, the GWP is expected to be high in flat and pit areas (Huaajie et al. 2016).

Fig. 13 Distances from the lineaments, where the distance unit is meter

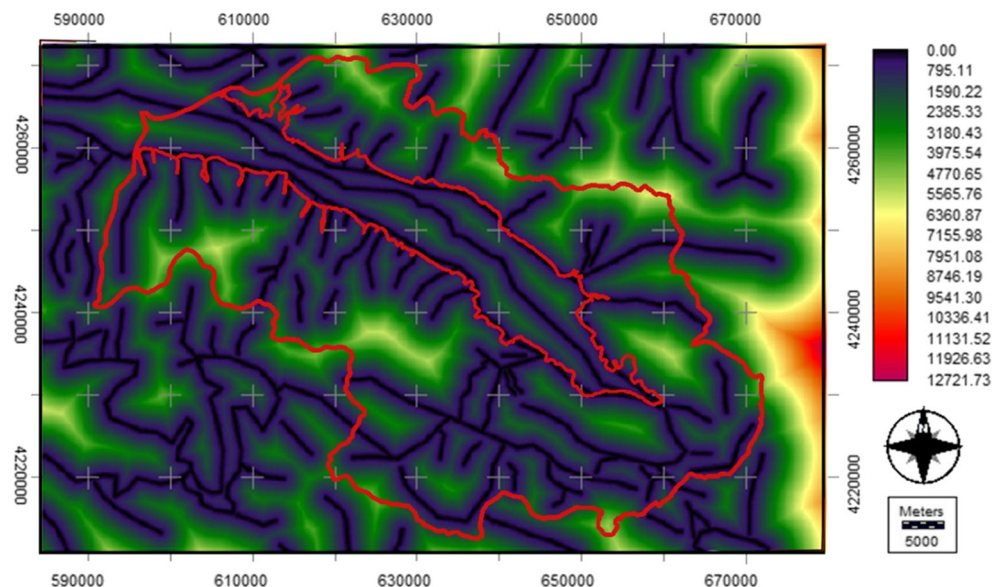
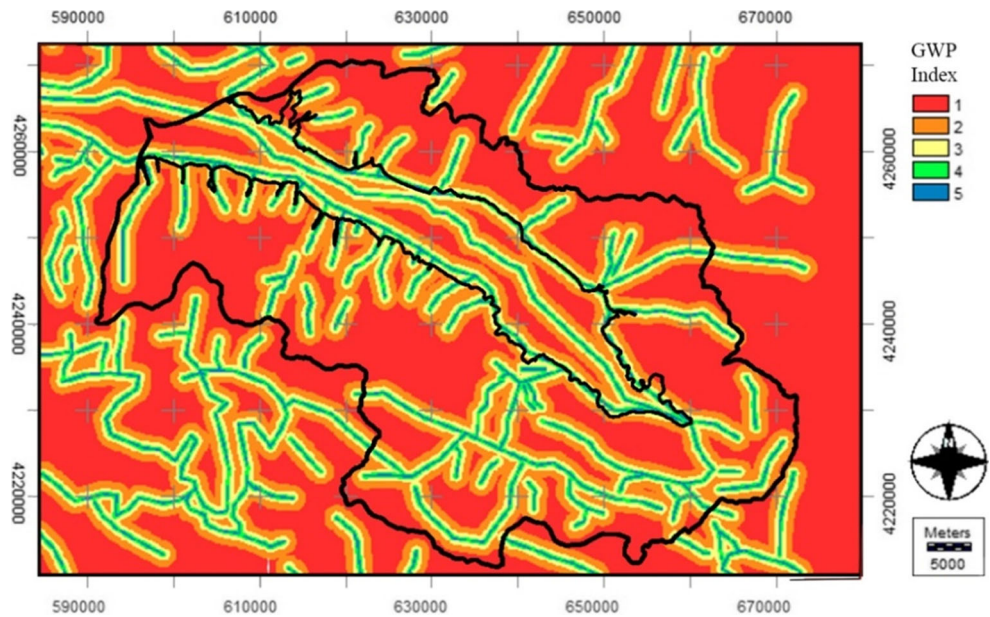


**Fig. 14** Classification of the lineament map (Fig. 13) with the index values of the GWP

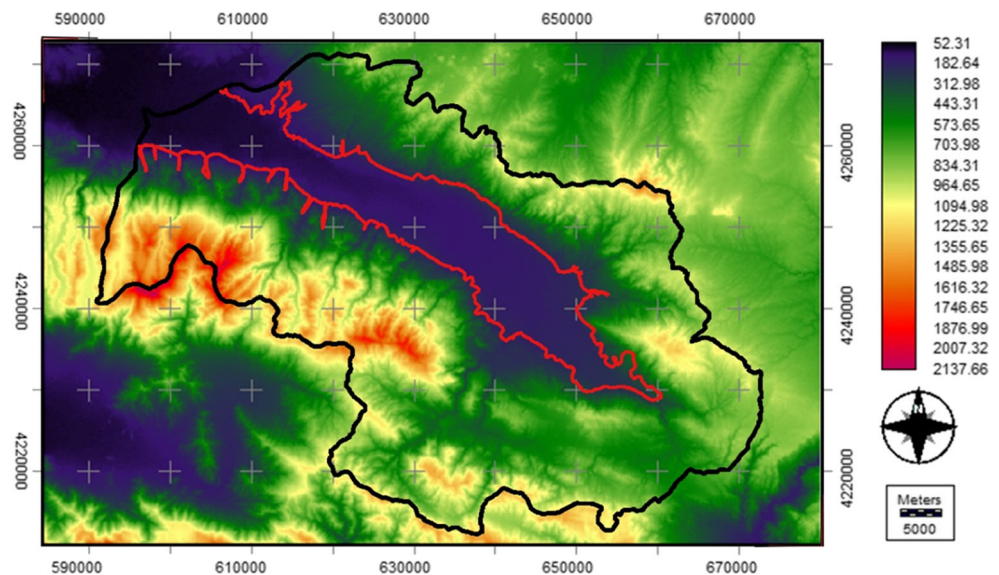


- Calculation method: the Aster DEM data was used for finding slope degrees and their analysis for classification (Figs. 17 and 18).
- The GWP decreases as the slope increases. For this reason, the GWP index value 5 was assigned to the lowest slope degree values and 1 point was assigned to the highest slope degree values. The weight coefficient of the slope proxy was assigned as 4 ( $W_6 = 4$ ) according to significance to the GWP (Figs. 17 and 18 and Table 1).

**Drainage—proxy 7**

Drainage networks (Figs. 19, 20, and 21) help identify the watershed and give an idea about the structural geology

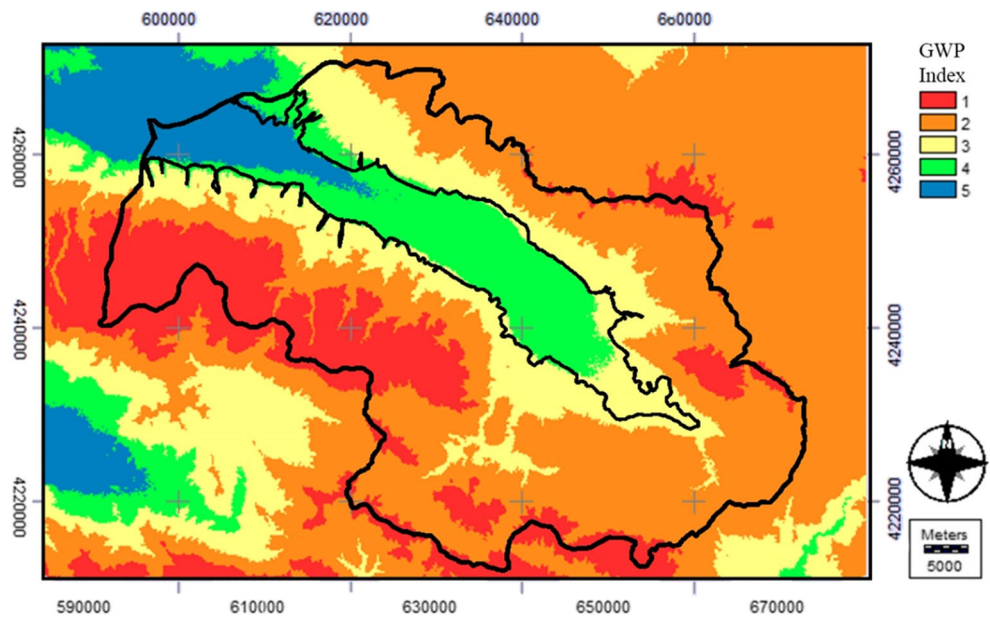
**Fig. 15** Topography (DEM) thematic map, where the elevation unit is meter



and determine the direction of the water flow. Besides, the types and densities of the drainages give information about the permeability of the soil. Thick drainage tissue is formed in porous and permeable rock formations, and thinner drainage tissues are formed in less permeable rocks (Waikar and Nilawar 2014).

- Calculation method: the Aster DEM data was used to extract the drainages using by the hydrology analysis tool in ArcGIS software (ArcGIS 2018). Then, drainages were imported into the Idrisi Selva system for further processes.
- The Gediz River and its surroundings have a GWP index value of 5, which is the highest value in the scoring because it has 1st degree drainage order hierarchy. After that, the Alaşehir Creek and its surroundings come with 4

**Fig. 16** Classification of the topography (DEM) thematic map (Fig. 15) with the index values of the GWP



points. The GWP index values increase as the stream order degree rank increases. The remaining areas have a value of 1. The weight coefficient of the drainage proxy was assigned as 4 ( $W_7 = 4$ ) according to significance to the GWP. Also, note that drainage lines were buffered with 200 m before the process. Instead, the distance operation could be applied from the drainages (Figs. 19, 20, and 21 and Table 1).

**Lithology—proxy 8**

Lithology (Figs. 22 and 23) describes the physical properties of the surface such as texture, color, and grain size. Physical

properties will affect the ability to infiltration, the amount of the groundwater. Lithology, in a sense, defines the porous permeability of the geological formation (Aneesh and Deka 2015). For example, while granular structures show more permeable properties, structures such as rock and clay soils show less permeable property.

- Calculation method: lithology data obtained from the TUBITAK Project (2018) was classified for getting the GWP index values.
- The GWP index value 1 for the rocks which have less permeability was assigned to rocks with Paleozoic and Neogene features. The GWP index value 2 was assigned to jointed rock areas. Areas with lakes and puddles were

**Fig. 17** Slope thematic map, where the slope unit is degree

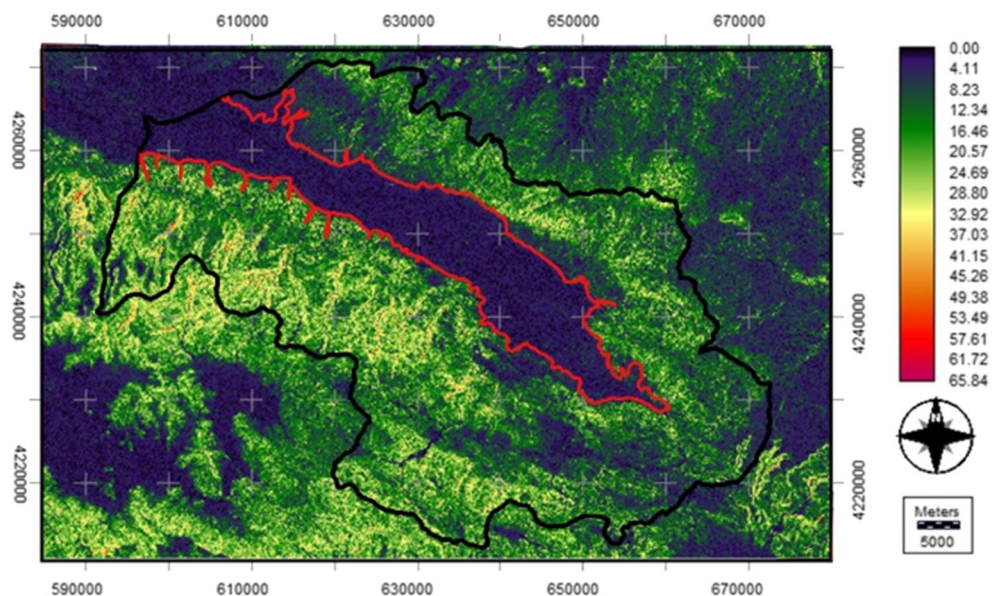
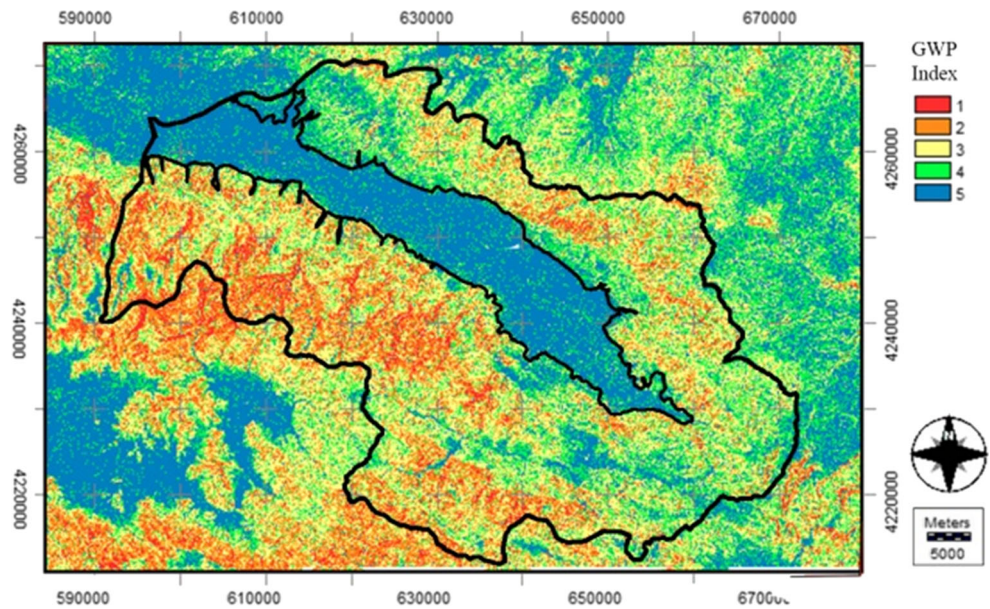


**Fig. 18** Classification of the slope thematic map (Fig. 17) with the index values of the GWP



assigned to the GWP index value 5, and value 4 was assigned to granular units. The karstic rocks were assigned to 3 points. The weight coefficient of the lithology proxy was assigned as maximum value, 5 ( $W_8 = 5$ ) according to significance to the GWP (Figs. 22 and 23 and Table 1).

groundwater in the region and the water conductivity of the aquifer material (Ahmed et al. 2017 and Bear 2007). Therefore, the high hydraulic conductivity value means more GWP in the region. In particular, the high hydraulic conductivity value lies in the border of the alluvial soils, which can be called as the aquifer border.

**Hydraulic conductivity—proxy 9**

The hydraulic conductivity (Figs. 24 and 25) is the proportionality constant that defines the liquid flow in an environment dependent on permeability and the physical properties of the aquifer. Hydraulic conductivity determines the velocity of

- Calculation method: hydraulic conductivity data obtained from the TUBITAK Project (2018) was classified for getting the GWP index values.
- The highest hydraulic conductivity values were assigned to the GWP index value 5 and the smallest values were assigned to 1 point (Table 1). The weight coefficient of the

**Fig. 19** Drainage thematic map

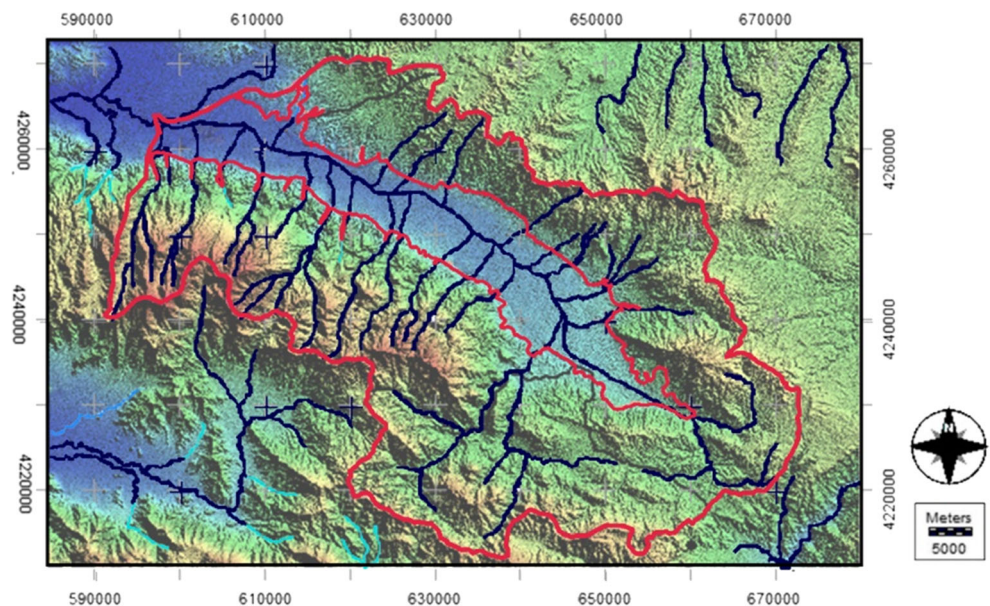
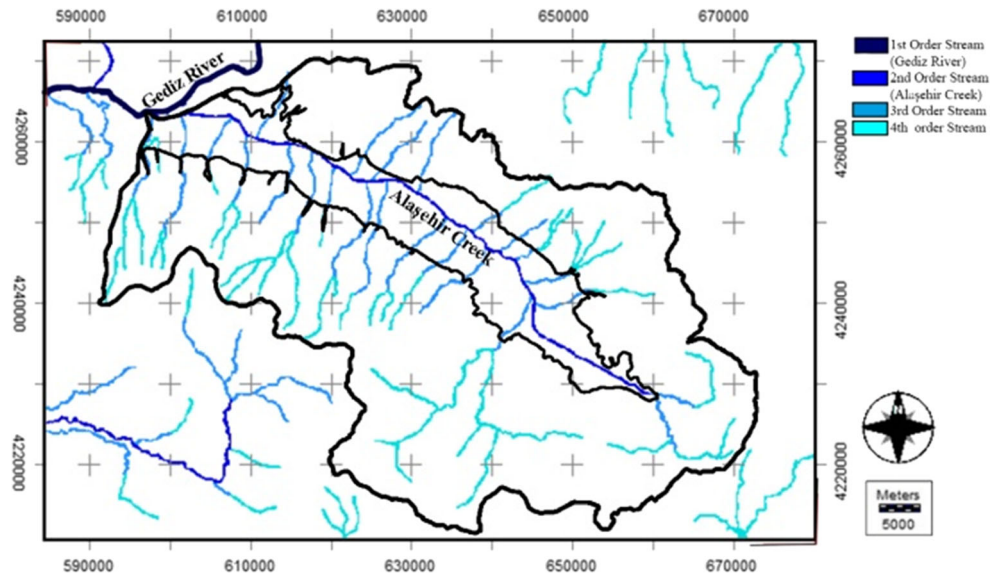


**Fig. 20** The drainage thematic map in the Strahler hierarchical order



hydraulic conductivity proxy was assigned as 4 ( $W_9 = 4$ ) according to significance to the GWP. The hydraulic conductivity unit is meter/day.

**Soil types—proxy 10**

Different types of soils (Figs. 26 and 27) have different permeability, structure, and drainage. These affect groundwater levels. Soil classification in this section is based on land-use capability classification system.

The first-class soils have less slope than 1% and have good drainage, permeability, and water holding capacity. The

second-class soils are slightly more inclined than the first-class soils. The third-class soils have a moderate slope but the water holding capacity is lower than the first and second-class soils. The fourth-grade soils are highly inclined and have poor drainage. The fifth-class soils are soils that have a slope of less than 1% and can be found in forested areas. The sixth-grade soils are too sloped, too wet, or too dry. Seventh-grade soils are more sloping, dry, or swampy soils. Eighth-grade soils serve as a catchment basin.

- Calculation method: soil type data obtained from both the DSI (2018) and TOB (2018) was classified for getting the GWP index values.

**Fig. 21** Classification of the hierarchical drainage map (Fig. 20) with the index values of the GWP

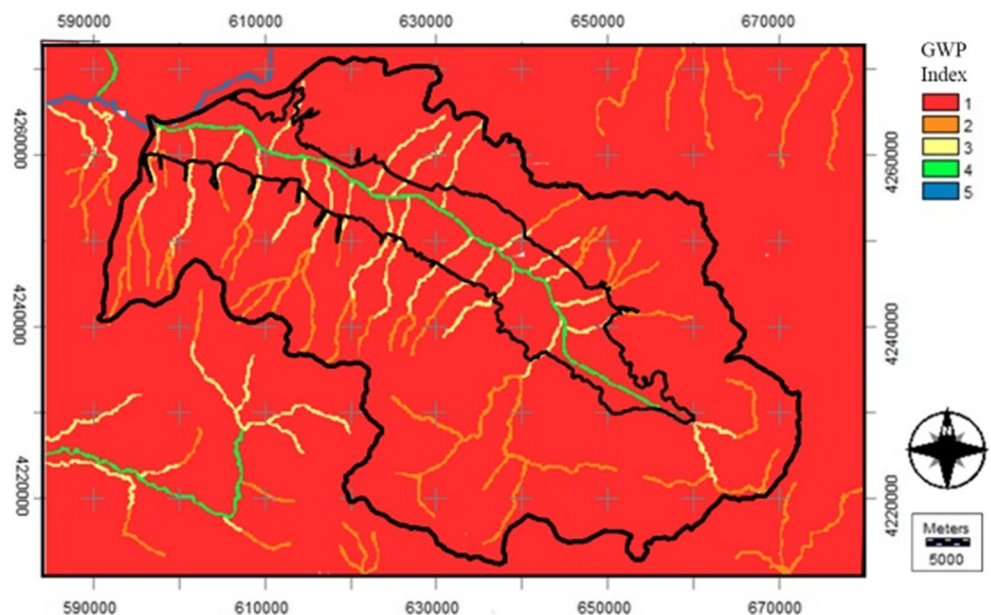
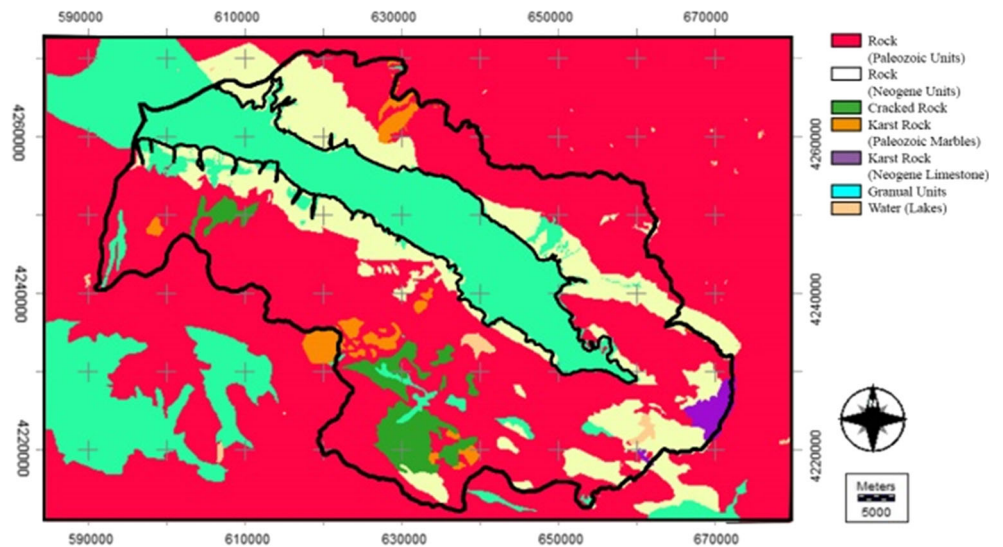




Fig. 22 Lithology thematic map



- The classification for the GWP index values is as that the first-, fifth-, and eighth-class soils have the GWP index value 5, the second- and the third-class soils have 4 points, the fourth- and sixth-class soils have 3 points, the second-class soils have 2 points, and the remaining areas have 1 point. The weight coefficient of the proxy of soil types was assigned as 2 ( $W_{10} = 2$ ) according to significance to the GWP (Figs. 26 and 27 and Table 1).

southeast of the study region. Based on these results, it is understood that the significant groundwater potential (GWP) and groundwater pollution risk (GWPR) areas are near the big settlement districts such as Alaşehir and Salihli. In particular, the 115-ha organized industrial zone located in the Salihli district is an important factor of the potential for consuming and contaminating water resources. Therefore, the study is so important for the selection of city and industrial areas as well as regional environmental planning in terms of the GWPR management.

**Results and discussion**

The result of the study (Figs. 28, 29, 30, and 31) indicates that the most GWP areas in the basin are seen in the west and

In this section, the final output image, the GWP is visualized and interpreted for decision-making. Comparing the final image with the available existing groundwater level data, the accuracy and efficiency of the method are seen consistent.

Fig. 23 Classification of the lithology thematic map (Fig. 22) with the index values of the GWP

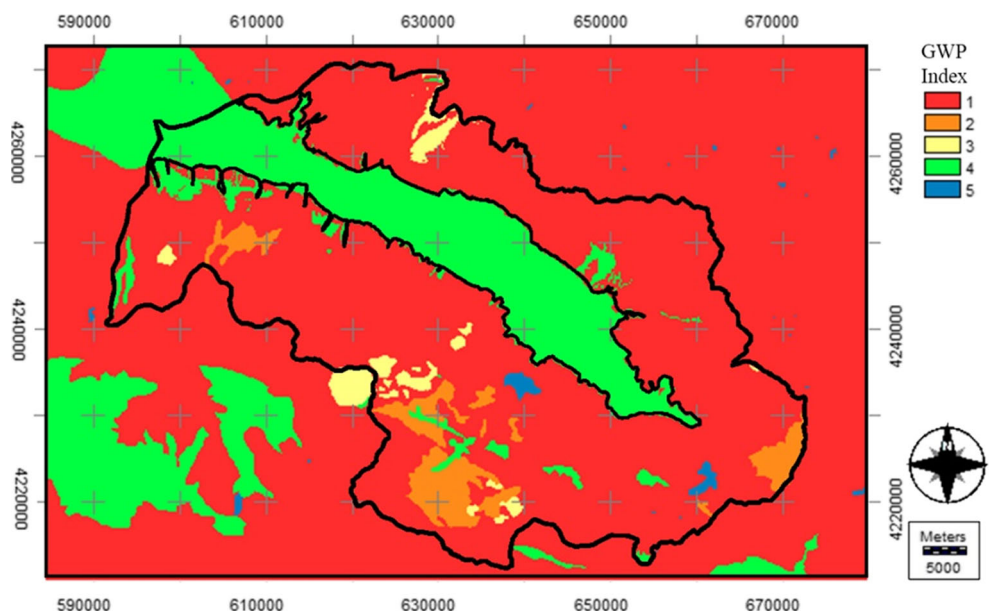
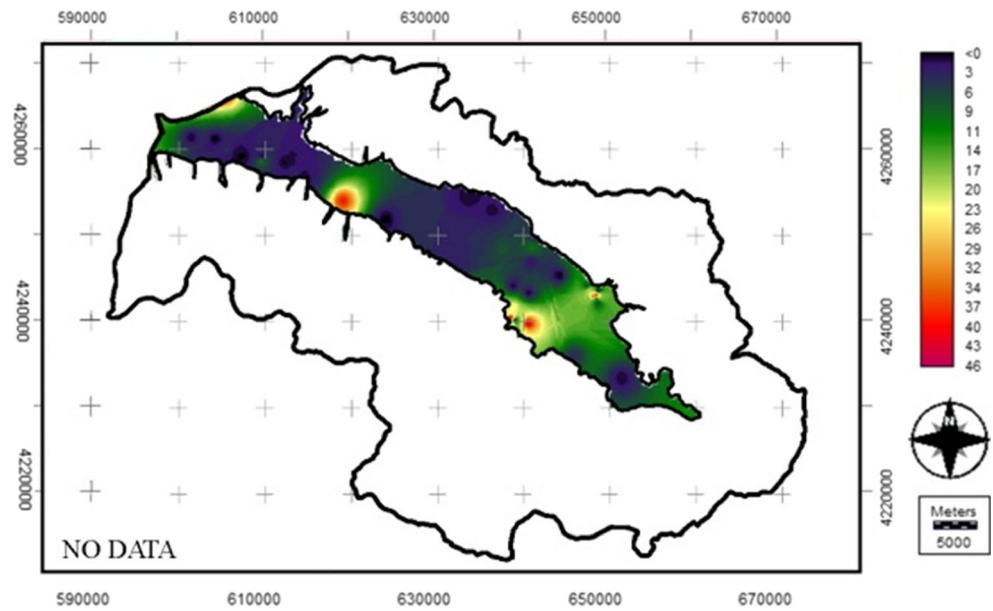


**Fig. 24** Hydraulic conductivity thematic map, where the hydraulic conductivity unit is meter/day



All the GWP index maps (Figs. 28, 29, and 30) were generated and visualized as well as interpreted by using all the ten proxies. Then, the summed image map of all the ten GWP maps (Fig. 29) was computed by the raster calculator tool in GIS.

The resultant final GWP map (Fig. 30) was obtained by the reclassification of summation of the GWP index maps of all the ten proxies, where the pixel values range from 30 to 121 (Fig. 29). The pixels with a value of 30 indicate areas with the lowest GWP, and those with a value of 121 indicate areas with the highest GWP. Therefore, this final image was reclassified into the five GWP index values as

categories of (1) very low, (2) low, (3) moderate, (4) high, and (5) very high (Fig. 30 and Table 1).

The study indicates that the best proxy for detecting the GWP is the drainage, as the worst proxy is the MNDWI. Therefore, the MNDWI proxy may be ignorable for the further studies. But, the study indicates that the drainage proxy is a must for the future works.

When interpreting the final GWP image map (Fig. 30), it may say that the areas having the highest GWP index values are the drainage areas within the alluvial boundary, namely the aquifer and the Alaşehir Creek surroundings. Higher GWP index values are observed within the alluvial

**Fig. 25** Classification of the hydraulic conductivity thematic map (Fig. 24) with the index values of the GWP

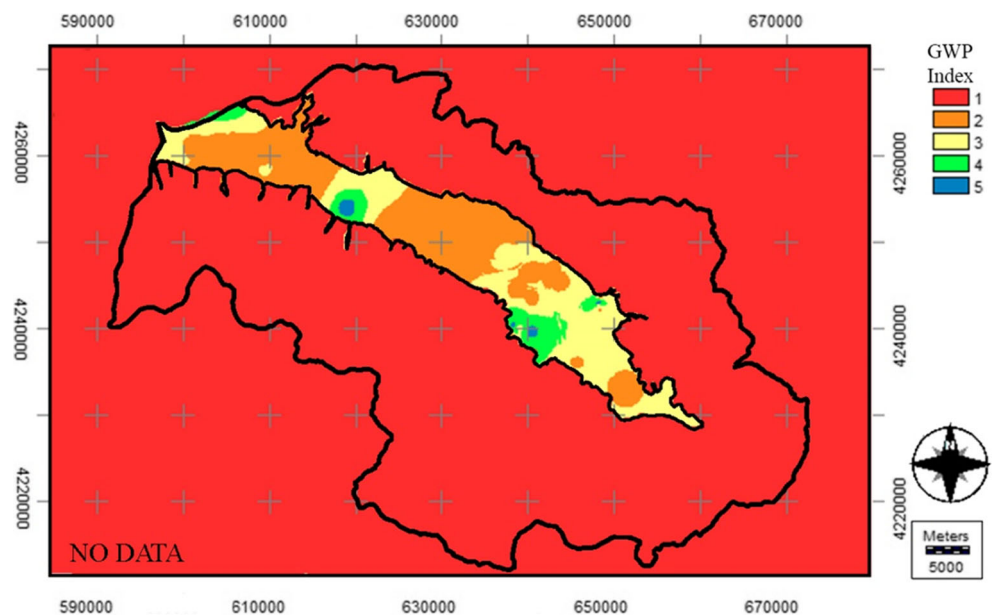
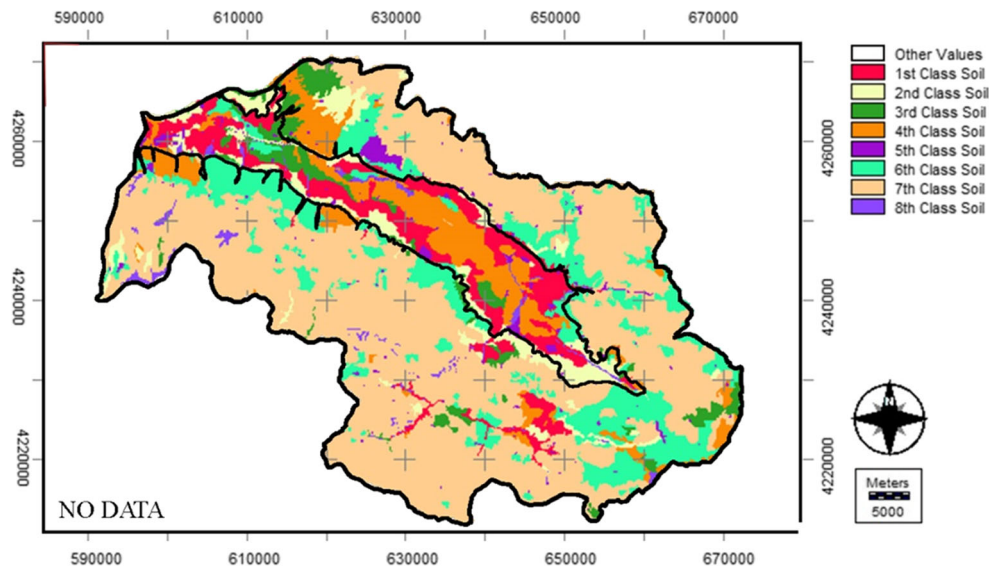


**Fig. 26** Soil type thematic map (DSI 2018; TOB 2018)



boundary. For comparison of the GWP map with the LULC thematic map (Fig. 10), when interpreting the output images of the study, the land-use classification image map of the study area looks like consistent with previous information data.

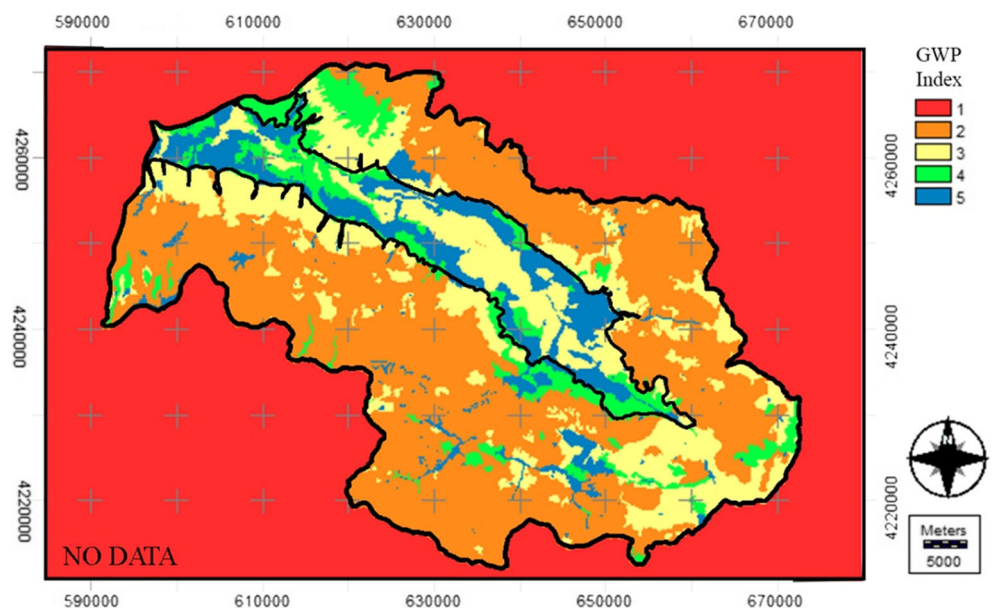
Currently, the settlements in the basin have been established mostly within the alluvial boundary, namely within the aquifer where the GWP is high. These regions can be listed as northeast of Salihli, southeast of Alaşehir, and around Dereköy. Generally, agricultural lands are concentrated in the areas within the alluvial border. It is seen that the most productive agricultural lands are located near the settlements of Salihli and Alaşehir. These areas have very high GWP index values.

In addition, in the south of the area, there is high GWP in the region outside the Alaşehir Basin. In this area, just like areas within the alluvial border, the ground consists of granule units. Besides, elevation and slope are suitable for groundwater.

In the south of the alluvial boundary, it is observed that the forested areas are dense. Although the forest areas are dense, the GWP in this section is lower than the area within the alluvial boundary. This is because the slope and elevation in this region is higher. Besides, it is possible to mention the effect of soil types and lithology in this area.

Areas with the lowest GWP are marked as bare rocks in the LULC thematic map. These areas are poor in

**Fig. 27** Classification of the soil type thematic map (Fig. 26) with the index values of the GWP



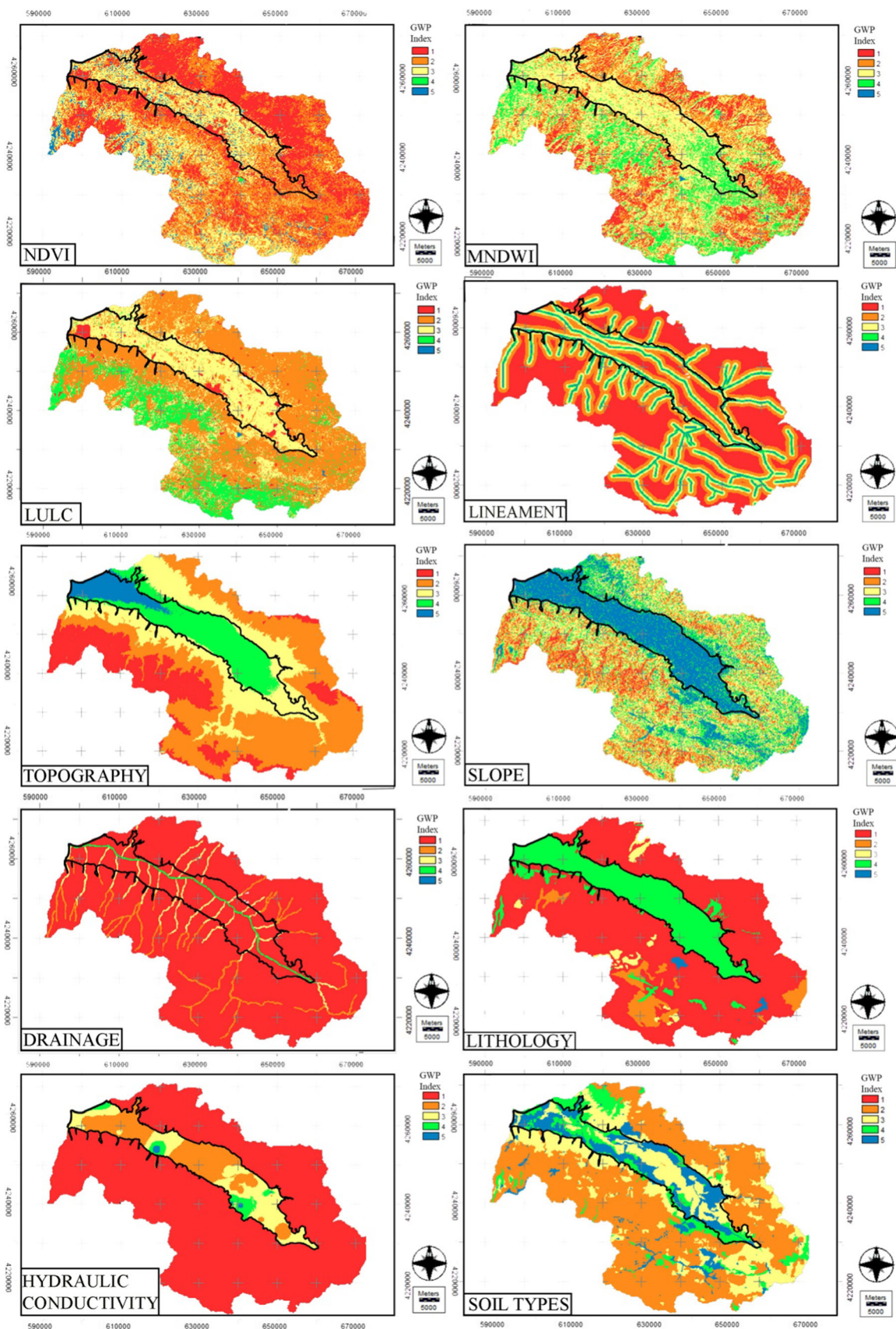
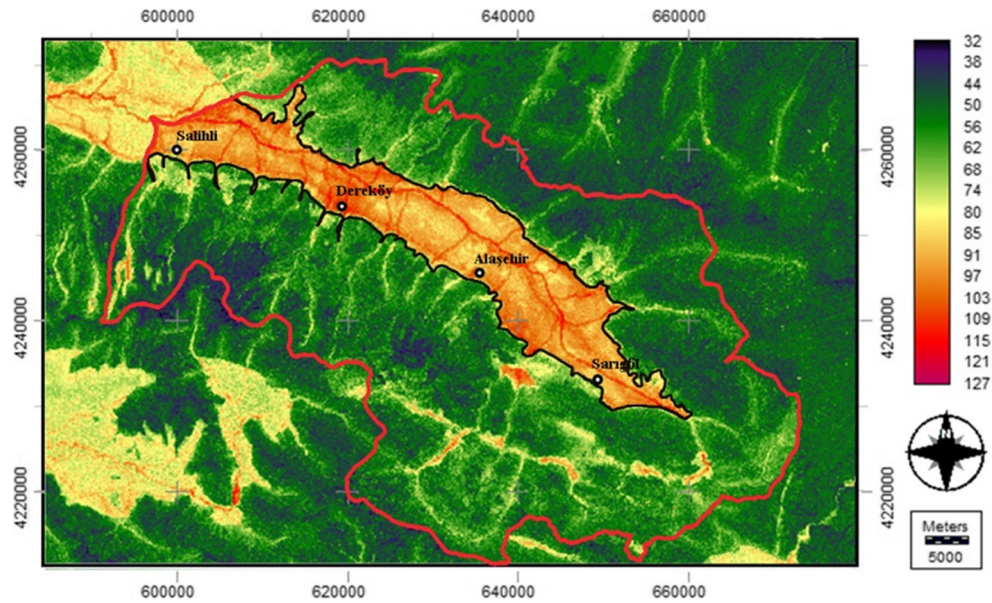


Fig. 28 Classification maps for each of all the ten proxies with the sub-basin border and the index values of the GWP

**Fig. 29** Summed groundwater potential (GWP) thematic map as the weighted image overlay using all the ten proxies



vegetation. In addition, the soil is weak in terms of permeability and surface texture is not very suitable to accumulate groundwater.

Alaşehir, Salihli, and Dereköy districts within the alluvial border have the highest GWP. These settlements are urban areas that have impacts on groundwater resources. In particular, the 115-ha organized industrial zone located in the Salihli district is an important factor of the potential for consuming and contaminate water resources (Fig. 31). Figure 31 shows the groundwater pollution risk because of both the industrial areas and settlements in the basin. Besides, the villages, agricultural lands, and forest areas in the region are directly related

to the water condition. Degradation of the quality of the groundwater presence and excessive consumption of water under the pressure of settlement and industry in the region will also reduce the quality and quantity of agricultural products. In addition, as a result of the plans and applications made without considering the presence of groundwater, damage will occur in buildings and infrastructure units, which will increase the cost. In this case, the prerequisite for ensuring the sustainability of economic development, agricultural production, and efficient use of groundwater resource in the region that has very high GWP in the Gediz River basin should be carefully evaluated.

**Fig. 30** Classification of the weighted image overlay (Fig. 29) with the index values of the GWP

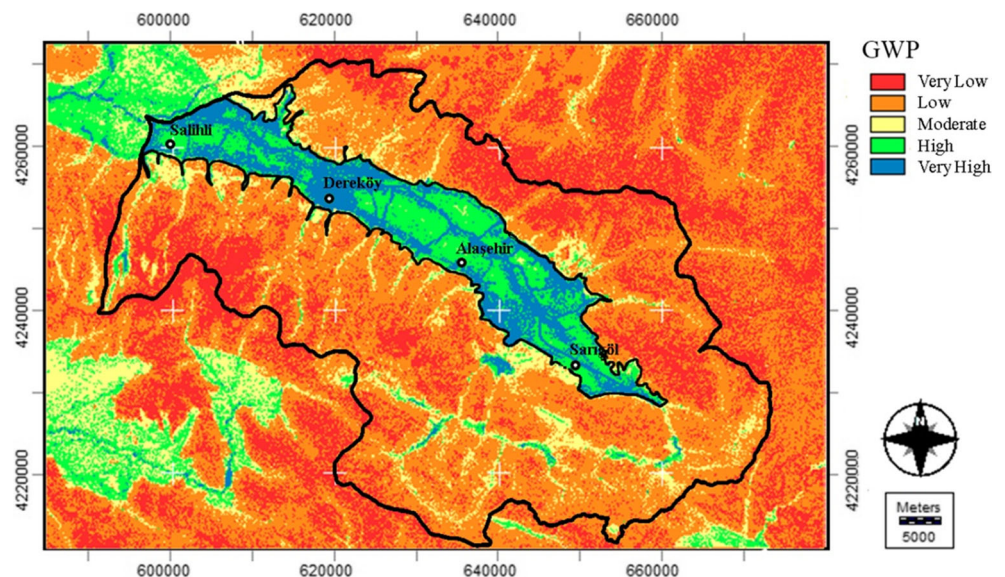
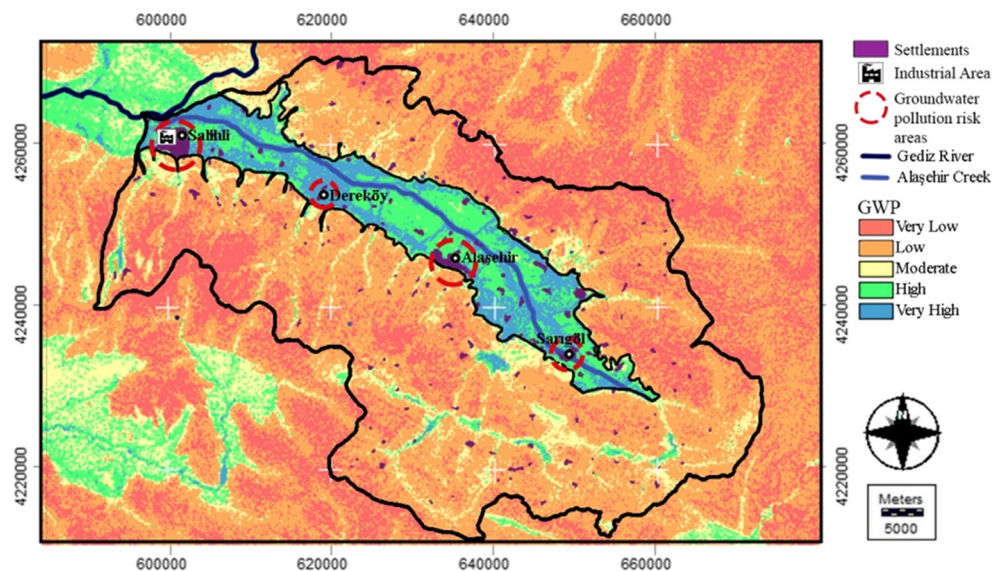


**Fig. 31** Groundwater pollution risk (GWPR) map with the industrial settlements areas



## Conclusions

The determination of the groundwater potential (GWP) is a big problem in the semi-arid regions because the water resources depend on the environmental, political, social, and economic issues. Many geological and environmental parameters play an important role in determining the GWP and GWPR areas of the alluvial aquifers. Therefore, The GIS is an indispensable tool for the evaluation of these parameters together. The final resultant map gives some opportunities for an easy understanding of the GWP and GWPR areas, and management and expanding areas of settlements on alluvial plains. It also indicates the most suitable site for the industrial area for assessing the overall parameters. In this regard, the multi-criteria (weighted image overlay) method, used for this study area, was applied for the determination of the GWP areas.

In the study, first of all, the general properties of the alluvial aquifer were investigated. The existence of multiple factors affecting the presence of the groundwater directed the study to use the multi-criteria decision-making method. According to this result, it can be said that the results of the study are generally informative and satisfactory.

According to this analysis, it has found out that the GWP zone in the aquifer is high to very high and mostly suitable for the GWP. When the pollution risk was considered, all of the Alaşehir alluvial aquifers show high to very high pollution risk and big settlement districts such as Alaşehir and Salihli locations on a very high pollution risk zone. This study showed that this wrong selection of settlement areas could influence the groundwater quality within the big GWP zone. Especially, the big industrial sites located in a very high pollution risk zone and that might cause groundwater pollution within the alluvial aquifer. This study showed that alluvial aquifer consisting of the big GWP zone should be protected from the industrial and settlement areas for the next generation.

Units such as residential areas and industrial facilities, located in the areas with the high GWP, are directly affected by the groundwater and also directly affecting the GWP, vice versa. This situation may endanger both the local GWP and the health of the people of the basin with an uncontrolled planning approach. In this context, it is important to ensure the construction and land-use restriction in the areas with high GWP and to prevent uncontrolled well drilling. The use of areas with high infiltration as a garden, recreation, or agricultural area will be more useful for the presence of the groundwater. Also, it can be possible to increase the production efficiency in the villages and other agricultural settlements, but only if the groundwater and surface water presence are analyzed correctly and shaping the existing and future plan decisions.

The study method and the results are therefore so important for the selection of city and industrial areas as well as regional environmental planning in terms of the GWPR management for future studies.

**Funding information** This study was supported by the Scientific and Technological Research Council of Turkey (TUBITAK), Project number: 114Y065.

## References

- Ahmed I, Nazzal Y, Zaidi F (2017) Groundwater pollution risk mapping using modified DRASTIC model in parts of Hail region of Saudi Arabia. *Environ Eng Res* 23(1):84–91. <https://doi.org/10.4491/eer.2017.072>
- Aneesh A, Deka PC (2015) Groundwater potential recharge zonation of Bengaluru urban district - a GIS-based analytic hierarchy process (AHP) technique approach. *Int Adv Res J Sci, Eng Technol* 23(1): 129–136. <https://doi.org/10.17148/IARJSET.2015.2628>
- ArcGIS (2018) Computer software manual. ESRI, Redlands <https://www.arcgis.com>

- Ardakani AHH, Ekhtesasi MR (2016) Groundwater potentiality through analytic hierarchy process (AHP) using remote sensing and geographic information system (GIS). *J Geopersia* 3(1):75–88
- Atlı A (2010) Yeraltı suyu (YAS) Kirlenme potansiyelinin CBS tabanlı DRASTIC modeli kullanılarak belirlenmesi ve Erzin ovası YAS hassasiyet haritalarının geliştirilmesi. PhD Thesis, Çukurova Üniversitesi, Adana. In Turkish
- Baba A, Sözbilir H (2012) Source of arsenic based on geological and hydro geochemical properties of geothermal systems in western Turkey. *Chem Geol* 334:364–377. <https://doi.org/10.1016/j.chemgeo.2012.06.006>
- Baba A, Gündüz O, Şimşek C, Elçi A, Murathan A, Sözbilir H (2016) High arsenic levels in groundwater resources of Gediz, Western Turkey. In: *Arsenic research and global sustainability*, AS2016 Proceedings, 19–23 June 2016, Stockholm, Sweden, pp 35–36
- Barış N (2008) Tahtalı barajı havzasının hidro jeolojik incelenmesi, ve yeraltı suyu kirlenabilirliğinin AHS-DRASTIC yöntemi ile değerlendirilmesi. PhD Thesis, Dokuz Eylül Üniversitesi, İzmir. In Turkish.
- Barsi J, Lee K, Kvaran G, Markham B, Pedelty J (2014) The spectral response of the Landsat-8 operational land imager. *Remote Sens* 10: 10232–10251. <https://doi.org/10.3390/rs61010232>
- Bear J (2007) *Hydraulics of groundwater*. Dover Publications, New York
- Carmon N, Shamir U, Pistiner SM (1997) Water-sensitive urban planning: protecting groundwater. *J Environ Plan Manag* 40(4):413–434. <https://doi.org/10.1080/09640569712010>
- COB (2008) Gediz havzası koruma eylem planı çalışması, Çevre Ve Orman Bakanlığı, Turkey. Çevre Yönetimi Genel Müdürlüğü, Su ve Toprak Yönetimi Dairesi, (in Turkish)
- Demirkesen AC, Evrendilek F (2017) Compositing climate change vulnerability of a Mediterranean region using spatiotemporally dynamic proxies for ecological and socioeconomic impacts and stabilities. *Environ Monit Assess* 189:29
- Dhar A, Sahoo S, Mandal U, Dey S, Bishi N, Kar A (2015) Hydro-environmental assessment of a regional ground water aquifer: Hirakud command area (India). *Environ Earth Sci* 73:4165–4178
- DSI (2016) Master plan of Gediz Graben, State water works (Devlet su işleri – DSI). Turkey (In Turkish)
- DSI (2018) Groundwater resources of Gediz Graben, State Water Works - (Devlet su işleri – DSI), Turkey, (In Turkish)
- Fashae OA, Tijani MN, Talabi AO, Adedeji OI (2013) Delineation of groundwater potential zones in the crystalline basement terrain of SW-Nigeria: an integrated GIS and remote sensing approach. *Appl Water Sci* 1(4):19–38. <https://doi.org/10.1007/s13201-013-0127-9>
- Frans VDV (1999) Impact of groundwater on urban development in the Netherlands. In: *Impacts of urban growth on surface water and groundwater quality*, pp.13-21. Proceedings. Birmingham: IUGG 99 Symposium HS5.
- Fu B, Burgher I (2015) Riparian vegetation NDVI dynamics and its relationship with climate, surface water and groundwater. *J Arid Environ* 113:59–68. <https://doi.org/10.1016/j.jaridenv.2014.09.010>
- Ghodratbadi S, Feizi F (2015) Identification of groundwater potential zones in Moalleman, Iran by remote sensing and index overlay technique in GIS. *Iran J Earth Sci* 2(7):142–152
- Hayat E, Baba A (2017) Quality of groundwater resources in Afghanistan. *Environ Monit Assess* 189:318
- Huajie D, Zhengdong D, Feifan D (2016) Classification of groundwater potential in chaoyang area based on QUEST algorithm. *IEEE Int Geosci Remote Sens Symp (IGARSS)*. <https://doi.org/10.1109/igarss.2016.7729225>
- Idrisi Selva (2018) Computer software manual. Clark labs, Clark university, 950 Main St. Worcester MA 01610 USA
- Jin XM, Schaepman ME, Clevers JGPW, Su BZ, Hu GC (2011) Groundwater depth and vegetation in the Ejina area, China. *Arid Land Res Manag* 2(25):194–199. <https://doi.org/10.1080/15324982.2011.554953>
- Landsat-8 OLI (2018) Landsat-8 operational land imager (OLI). Multi-spectral satellite image bands. USGS earth explorer. <https://earthexplorer.usgs.gov>
- Mandal U, Sahoo S, Munusamy SB, Dhar A, Panda SN, Kar A, Mishra PK (2016) Delineation of groundwater potential zones of coastal groundwater basin using multi-criteria decision making technique. *Water Resour Manag* 12(30):4293–4310. <https://doi.org/10.1007/s11269-016-1421-8>
- Mc Feeters SK (1996) The use of the normalized difference water index (NDWI) in the delineation of open water features. *Int J Remote Sens* 7(17):1425–1432. <https://doi.org/10.1080/01431169608948714>
- Ndatuwong LG, Yadav GS (2014) Integration of hydrogeological factors for identification of groundwater potential zones using remote sensing and GIS techniques. *J Geosci Geomat* 1(2):11–16. <https://doi.org/10.12691/jgg-2-2>
- Özen T, Bülbül A, Tarcan G (2012) Reservoir and hydro geochemical characterizations of geothermal fields in Salihli, Turkey. *J Asian Earth Sci* 60:1–17. <https://doi.org/10.1016/j.jseaes.2012.07.016>
- Qiao X, Zhao C, Shao Q, Hassan M (2018) Structural characterization of corn stover lignin after hydrogen peroxide presoaking prior to ammonia fiber expansion pretreatment. *Energy Fuel* 32(5):6022–6030
- Rabet RS, Şimşek C, Baba A, Murathan A (2017) Blowout mechanism of Alaşehir (Turkey) geothermal field and its effects on groundwater chemistry. *Environ Earth Sci* 76:49. <https://doi.org/10.1007/s12665-016-6334-6>
- Ramu BM, Vinay M (2015) Identification of ground water potential zones using GIS and remote sensing techniques: a case study of Mysore Taluk Karnataka. *Int J Geomat Geosci* 3:393–403
- Saaty TL (1980) *The analytic hierarchy process (AHP)*. McGraw-Hill, New York
- Saaty TL (2008) Decision making with the analytic hierarchy process (AHP). *Int J Serv Sci* 1(1):83–98
- Saaty TL (2012) Decision making for leaders: the analytic hierarchy process (AHP) for decisions in a complex world. Third, revised edn. RWS Publications, Pittsburgh
- Seyitoğlu G, Çemen İ, Tekeli O (2000) Extensional folding in the Alaşehir (Gediz) graben, western Turkey. *J Geol Soc* 6(157):1097–1100. <https://doi.org/10.1144/jgs.157.6.1097>
- TOB (2018) Toprak ve Arazi Sınıflaması Standartları Teknik Talimatı, Tarım ve Orman Bakanlığı (TOB), Turkey. (In Turkish).
- TUBITAK Project (2018) Alaşehir alt havzası yeraltı suyu besleniminin akifer bazlı izlenmesi - CBS tabanlı alansal yeraltı suyu beslenim haritasının oluşturulması. Project No:115Y065, (In Turkish)
- Velibeyoğlu K, Yazdani H, Baba A (2018) Groundwater in local development strategies: case of Izmir, WST. *Water Supply* 18:1339–1349. <https://doi.org/10.2166/ws.2017.199>
- Waikar ML, Nilawar AP (2017) Identification of groundwater potential zone using remote sensing and GIS technique. *Int J Innov Res Sci, Eng Technol* 5(3):12163–12174
- Xu H (2006) Modification of normalized difference water index (MNDWI) to enhance open water features in remotely sensed imagery. *Int J Remote Sens* 14(27):3025–3033. <https://doi.org/10.1080/01431160600589179>
- Zhao C, Qiao X, Cao Y, Shao Q (2017) Application of hydrogen peroxide presoaking prior to ammonia fiber expansion pretreatment of energy crops. *Fuel* 205:184–191. <https://doi.org/10.1016/j.fuel.2017.05.073>